Synthesis, biological evaluation and molecular docking of novel chalcone–coumarin hybrids as anticancer and antimalarial agents

ARTICLE *in* EUROPEAN JOURNAL OF MEDICINAL CHEMISTRY · OCTOBER 2014

Impact Factor: 3.45 · DOI: 10.1016/j.ejmech.2014.07.087

European Journal of Medicinal Chemistry 85 (2014) 65–76

Contents lists available at ScienceDirect

European Journal of Medicinal Chemistry

journal homepage: http://www.elsevier.com/locate/ejmech

Original article

Synthesis, biological evaluation and molecular docking of novel chalcone–coumarin hybrids as anticancer and antimalarial agents

Ratchanok Pingaew [a, *], Amporn Saekee [a], Prasit Mandi [b, c], Chanin Nantasenamat [b, c], Supaluk Prachayasittikul [b], Somsak Ruchirawat [d, e, f], Virapong Prachayasittikul [c]

[a] Department of Chemistry, Faculty of Science, Srinakharinwirot University, Bangkok 10110, Thailand
[b] Center of Data Mining and Biomedical Informatics, Faculty of Medical Technology, Mahidol University, Bangkok 10700, Thailand
[c] Department of Clinical Microbiology and Applied Technology, Faculty of Medical Technology, Mahidol University, Bangkok 10700, Thailand
[d] Chulabhorn Research Institute, Bangkok 10210, Thailand
[e] Program in Chemical Biology, Chulabhorn Graduate Institute, Bangkok 10210, Thailand
[f] Center of Excellence on Environmental Health and Toxicology (EHT), CHE, Ministry of Education, Thailand

ARTICLE INFO

Article history:
Received 13 March 2014
Received in revised form
19 July 2014
Accepted 24 July 2014
Available online 24 July 2014

Keywords:
Chalcone
Coumarin
Triazole
Molecular docking
Cytotoxicity
Antimalarial activity

ABSTRACT

A new series of chalcone–coumarin derivatives (**9**–**19**) linked by the 1,2,3-triazole ring were synthesized through the azide/alkyne dipolar cycloaddition. Hybrid molecules were evaluated for their cytotoxic activity against four cancer cell lines (e.g., HuCCA-1, HepG2, A549 and MOLT-3) and antimalarial activity toward *Plasmodium falciparum*. Most of the synthesized hybrids, except for analogs **10** and **16**, displayed cytotoxicity against MOLT-3 cell line without affecting normal cells. Analogs (**10**, **11**, **16** and **18**) exhibited higher inhibitory efficacy than the control drug, etoposide, in HepG2 cells. Significantly, the high cytotoxic potency of the hybrid **11** was shown to be non-toxic to normal cells. Interestingly, the chalcone–coumarin **18** was the most potent antimalarial compound affording IC_{50} value of 1.60 μM. Molecular docking suggested that the cytotoxicity of reported hybrids could be possibly due to their dual inhibition of α- and β-tubulins at GTP and colchicine binding sites, respectively. Furthermore, falcipain-2 was identified to be a plausible target site of the hybrids given their antimalarial potency.

1. Introduction

Chalcones (1,3-diaryl-2-propen-1-ones) belonging to the flavonoid class of natural products have drawn considerable interest owing to their pharmacological properties [1–6]. Naturally-occurring chalcones and their synthetic analogs displayed significant cytotoxic activity against various cancer cells. One of the most widely proposed anticancer mechanisms of chalcones is its prevention of tubulin polymerization by binding to the colchicine-binding site [5–7]. The natural chalcone, licochalcone A (Fig. 1), isolated from Chinese licorice roots was revealed to exhibit potential antimalarial activity [8]. Numerous chalcones have been extensively studied for their antimalarial activity, and the results showed that the activity was exerted by plasmodial aspartate protease [9], cysteine protease [10–12] and cyclin-dependent protein kinase (CDK), Pfmrk [13] inhibitors. In addition, inhibition of new permeation pathways induced by malarial parasite in the erythrocyte membranes have been disclosed [14]. Structure–activity relationship (SAR) elucidation of antimalarial chalcones demonstrated that the presence of the α,β-unsaturated ketone linker [11] and *E* configuration [15] are critical for their activities in which the alkoxylated chalcones displayed superior antimalarial activity than those of the hydroxylated analogs [14,16].

Pharmacological applications of synthetic and natural coumarins (Fig. 1) have previously been reviewed [17–20]. For example, 7-hydroxycoumarin was shown to inhibit the release of cyclin D1, which is overexpressed in many types of cancers [19]. Daphnetin, the Chinese herbal product, exhibited potency against malarial parasite both *in vitro* and *in vivo* [21].

The design and development of new bioactive agents based on the molecular hybridization strategy, involving the integration of two or more pharmacophoric units having different mechanisms of action in the same molecule, is a rationally attractive approach [22,23]. These combined pharmacophores probably offer some advantages such as in overcoming drug resistance [24] as well as improving their biological potency [25]. Such hybrid approaches had previously reported the coupling of chalcones with various bioactive compounds including nucleosides [26], quinolines

* Corresponding author.
E-mail address: ratchanok@swu.ac.th (R. Pingaew).

http://dx.doi.org/10.1016/j.ejmech.2014.07.087
0223-5234/

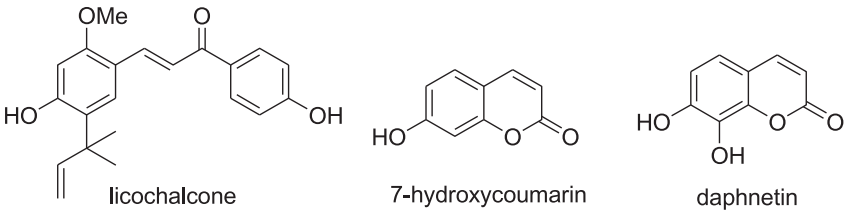

Fig. 1. Bioactive chalcone and coumarins.

[26–28], pyrrolobenzodiazepines [29], ciprofloxacin [30], β-lactam [31], nitric oxide donors [32,33], thiolactone [12] and isatin [12]. In addition, a number of new chalcone–coumarin hybrids affording anticancer, antimalarial, vasorelaxant, anti-inflammatory, antioxidant and trypanocidal activities have been documented [10,34–39]. For instance, hybrid (**1**) (Fig. 2) has been found to exert significant cytotoxic activity against the paclitaxel-resistant cancer cells [37]. Derivative (**2**) has shown cytotoxic activity against cervical carcinoma cells (IC_{50} = 3.59 μM) without affecting normal fibroblast NIH3T3 cells [38]. Additionally, conjugate (**3**) exhibited antimalarial activity against both chloroquine sensitive and chloroquine-resistant strains with IC_{50} values of 3.1 and 4 μg/mL, respectively [39]. Such chalcone analogs (**1**–**3**) constitute coumaryl group, but the different substituents are pyridyl and phenyl groups on the 2-propen-1-one core structure.

Triazole moiety is commonly found in diverse bioactive compounds. Its distinct property is its metabolically stable heterocyclic ring that is capable of forming hydrogen bonds. Furthermore, it can be used as linkers of various molecules as to give rise to new compounds and which might increase their bioavailability [40].

The reported cytotoxic and antimalarial activities of chalcone analogs led to our rational design and synthesis of new molecular hybrids of chalcone and coumarin tethered by the triazole ring. In this article, the synthetic approaches have been designed as follows (Fig. 3):

(i) use 1,3-diphenylpropenone (rings A and B) as the core structure
(ii) vary methoxy groups substituted on ring B (2,3-dimethoxy-, 3,4-dimethoxy-, 2,3,4-trimethoxy- or 3,4,5-trimethoxy substituents)
(iii) vary the position of 1,2,3-triazole ring on ring A (3- or 4-position)
(iv) vary coumaryl ring substituted on the triazole moiety (4-chromenone or 7-chromenone).

Herein, a variety of novel target chalcone–coumarin molecules containing triazole linker (**9**–**19**) were synthesized and evaluated for their cytotoxic and antimalarial activities. In addition, molecular docking studies of these compounds toward their target proteins, tubulin and falcipain-2, have been carried out to gain insight into the biological results.

2. Results and discussion

2.1. Chemistry

The novel target chalcone–coumarin hybrids (**9**–**19**) were synthesized in three steps (Scheme 1). Initially, chalcones **6** were synthesized using the base-catalyzed Claisen–Schmidt condensation of various aromatic aldehydes **4** with two aminoacetophenones **5** (3- or 4-NH_2). Subsequently, azotization reaction of the aminochalcones **6** using sodium nitrite and sodium azide in a mixture of glacial acetic acid and concentrated hydrochloric acid afforded the corresponding azidochalcones **7**. The azide/alkyne dipolar cycloaddition, represented as the Click-type reaction, is the key route to the synthesis of 1,2,3-triazole linkage. Finally, the azides **7** readily underwent cycloaddition with alkynes (**8**) to afford the novel desired hybrid molecules (**9**–**19**) in moderate to good yields (50–88%). The starting alkynes (**8**) were derived from the alkylation of either 4-hydroxycoumarin or 7-hydroxycoumarin with propargyl bromide.

Structures of the hybrids (**9**–**19**) were characterized by ^{1}H NMR spectra, which showed the existence of the singlet of methine proton at δ 8–10 ppm indicating that the triazole linkage was formed. In addition, triazole methylene ether linker displayed the singlet of methylene proton at δ 5–6 ppm. The chalcone part was shown to be in the *trans*-configuration of double bond as represented by the coupling constant (*J*) values of 15–16 Hz. Structures of all obtained compounds were further supported by ^{13}C NMR, IR and HRMS. Such spectral data using the chalcone–coumarin hybrid **9** as an example are provided below.

The hybrid **9** showed molecular ion $[M+Na]^+$ peak at 532.1464 corresponding to the molecular formula of $C_{29}H_{23}N_3NaO_6$. The IR spectra of the compound **9** exhibited absorption bands of C=O groups of coumarin and chalcone moieties at 1723 and 1660 cm^{-1}, respectively. In the ^{1}H NMR spectra, two singlets at δ 3.92 and 3.94 ppm were assigned to two methoxy protons on ring B of the chalcone part. The methylene protons connected to the triazole moiety appeared as a singlet at δ 5.35 ppm. Two protons of the

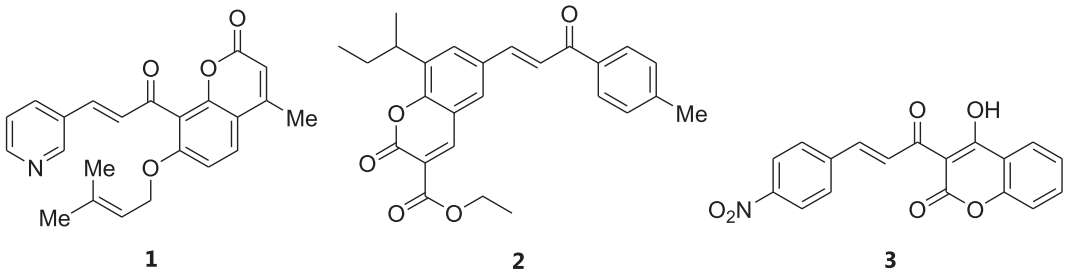

Fig. 2. Chalcone containing coumarin derivatives.

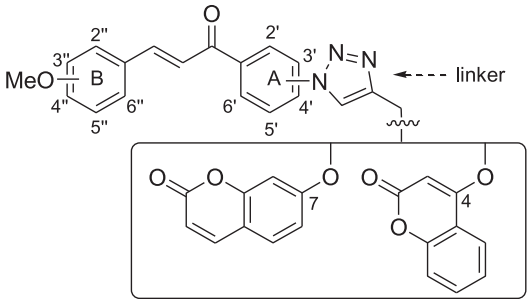

Fig. 3. Newly designed chalcone–coumarin hybrids linked by triazole.

propenone moiety were observed as two doublets at δ 7.38 and 7.82 ppm with J value of 15.6 Hz. Two doublets at δ 6.25 and 7.62 ppm with J value of 9.5 Hz were attributed to two protons of coumarin ring at positions 3 and 4. The rest of aromatic protons of this ring at C-6 and C-8 appeared as multiplet at δ 6.92–6.98 ppm, and a proton at position 5 was found to be displayed as a doublet at δ 7.39 ppm with J value of 8.9 Hz. The aromatic ring B protons of chalcone at position 5′, 2′′ and 6′′ were observed at δ 6.89 (d, J = 8.3 Hz), 7.16 (s) and 7.25 (d, J = 8.3 Hz) ppm, respectively. The aromatic protons at position 5′ and 2′ of chalcone (ring A) were visible as a triplet at δ 7.68 ppm with J value of 7.9 Hz and as a singlet at δ 8.32 ppm, respectively, whereas position 4′ and 6′ appeared as two doublets at δ 8.01 (J = 8.0 Hz) and 8.07 (J = 7.7 Hz) ppm. A singlet of a methine proton of the triazole ring appeared at δ 8.20 ppm. In the ^{13}C NMR spectra, two methoxy carbons (at C-3′′ and C-4′′) of chalcone part (ring B) were observed at δ 56.1 ppm whereas a methylene carbon adjacent to triazole ring was noted at 62.3 ppm. Two carbonyl groups of ketone and lactone were seen at 188.9 and 161.0 ppm, respectively. Nine quaternary aromatic carbons (ArC) were observed at chemical shift 113.2, 127.5, 137.3, 140.2, 144.1, 149.4, 151.9, 155.8 and 161.2 ppm. Eleven tertiary aromatic carbons (ArCH) and four olefinic carbons appeared at chemical shift 102.2, 110.3, 111.2, 112.7, 113.6, 119.0, 120.1, 121.3, 123.6, 124.3, 128.7, 129.0, 130.2, 143.2 and 146.5 ppm.

2.2. Biological activities

2.2.1. Cytotoxic activity

Cytotoxicity of the synthesized chalcone–coumarin hybrids (**9**–**19**) were assayed against human cancer cell lines; HuCCA-1 (cholangiocarcinoma), HepG2 (hepatocellular carcinoma), A549 (lung carcinoma) and MOLT-3 (lymphoblastic leukemia), as summarized in Table 1. These compounds were also evaluated for non-cancerous cell line (Vero) derived from African green monkey kidney.

Results showed that most of the tested hybrid molecules exerted significant cytotoxicity, especially against MOLT-3 cancer cell line, except for the hybrid **11**. Among these, triazole hybrid **16** was shown to be the most potent cytotoxic compound against MOLT-3 cells with an IC_{50} of 0.53 μM. Aside from MOLT-3 cells, compounds **9**–**11** and **15**–**17** also showed inhibitory effect against HuCCA-1 cells. However, tri-substituted methoxy hybrids **12**, **13**, **14** and **19** selectively inhibited MOLT-3 cells with IC_{50} in the range of 3.89–79.49 μM. Significant cytotoxic activity toward A549 cells was noted for 2,3-dimethoxy analogs **10**, **11** and **16**, in which **11** was the most potent compound (IC_{50} = 7.95 μM). The investigated chalcone–coumarin hybrids bear a variety of substituents on ring B (2,3-, 3,4-, 2,3,4- and 3,4,5-methoxys) and ring A (3- and 4-substituted triazoles) of the chalcone moiety while the coumarins linked to triazoles as a series of 7- (**9**–**14**) and 4- (**15**–**19**) substituted coumarins. SAR investigation of the compounds revealed that the most potent and promising cytotoxicity depended on the substitution pattern of substituents on rings A and B as well as coumaryl moieties. Apparently, compounds with 2,3-dimethoxy groups on ring B and 3-substituted ring A of 4-oxycoumaryl series exhibited higher inhibitory potency (HuCCA-1 cells) than the corresponding 3,4-dimethoxy (ring B) as observed for **16** (IC_{50} = 2.36 μM) and **15** (IC_{50} = 38.57 μM). Similar cytotoxic effect against HuCCA-1 was noted for 7-oxycoumaryl analogs **10** (IC_{50} = 11.13 μM) and **9** (IC_{50} = 33.37 μM). Obviously, 2,3-dimethoxy (ring B), 3-substituent (ring A) of 4-coumaryl analog **16** exerted higher cytotoxicity towards all of the tested cancer cells as compared to its 7-coumaryl analog (**10**). In addition, other 4-coumaryl derivatives exerted

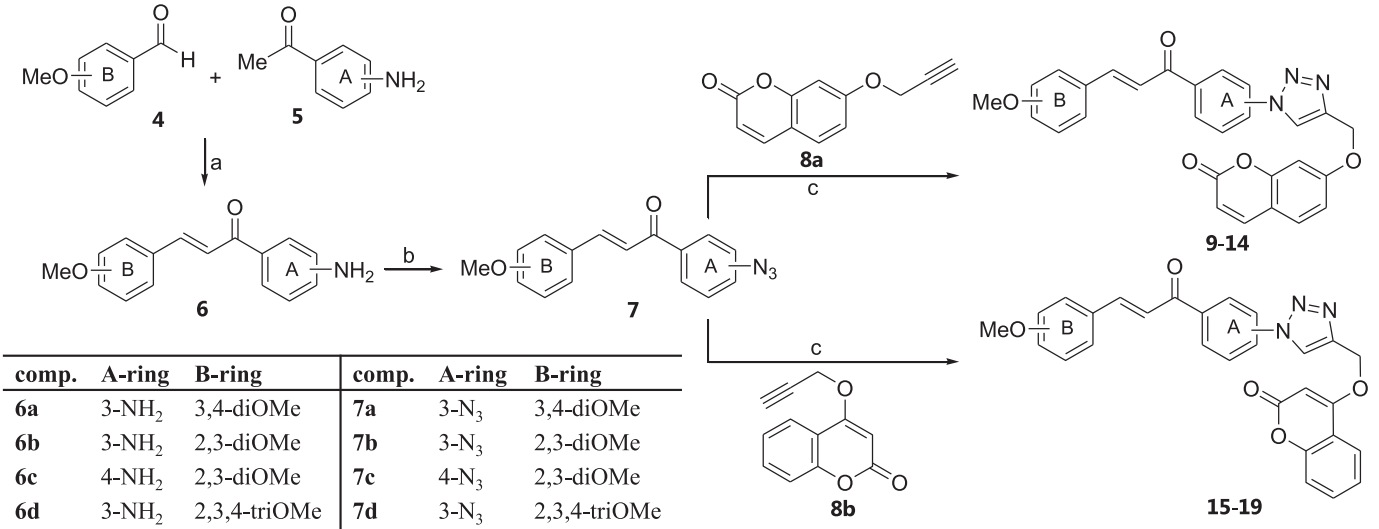

comp.	A-ring	B-ring	comp.	A-ring	B-ring
6a	3-NH_2	3,4-diOMe	**7a**	3-N_3	3,4-diOMe
6b	3-NH_2	2,3-diOMe	**7b**	3-N_3	2,3-diOMe
6c	4-NH_2	2,3-diOMe	**7c**	4-N_3	2,3-diOMe
6d	3-NH_2	2,3,4-triOMe	**7d**	3-N_3	2,3,4-triOMe
6e	4-NH_2	2,3,4-triOMe	**7e**	4-N_3	2,3,4-triOMe
6f	4-NH_2	3,4,5-triOMe	**7f**	4-N_3	3,4,5-triOMe

Reagents and conditions:
(a) 40% KOH, EtOH, rt
(b) $NaNO_2$, HCl/CH_3COOH, 0 °C, 15 min then NaN_3, rt, 30 min
(c) $CuSO_4 \cdot 5H_2O$, sodium ascorbate, t-$BuOH/H_2O$, rt

Scheme 1. Synthesis of chalcone–coumarin hybrids (**9**–**19**) through the Click reaction.

Table 1
Cytotoxic and antimalarial activities (IC_{50}, μM) of hybrid compounds (**9**–**19**).

Compound	A-ring	B-ring	Cancer cell lines[a]				Antimalarial[b]	Vero cell line
			HuCCA-1	HepG2	A549	MOLT-3		
9	3-Triazole	3,4-DiOMe	33.37 ± 0.84	Non-cytotoxic	Non-cytotoxic	3.12 ± 0.11	Inactive	Non-cytotoxic
10	3-Triazole	2,3-DiOMe	11.13 ± 0.40	15.70 ± 2.00	31.40 ± 1.00	5.16 ± 0.69	6.63	35.03
11	4-Triazole	2,3-DiOMe	4.81 ± 0.92	8.18 ± 0.76	7.95 ± 3.04	Non-cytotoxic	Inactive	Non-cytotoxic
12	3-Triazole	2,3,4-TriOMe	Non-cytotoxic	Non-cytotoxic	Non-cytotoxic	3.89 ± 0.28	13.03	Non-cytotoxic
13	4-Triazole	2,3,4-TriOMe	Non-cytotoxic	Non-cytotoxic	Non-cytotoxic	22.50 ± 3.63	Inactive	Non-cytotoxic
14	4-Triazole	3,4,5-TriOMe	Non-cytotoxic	Non-cytotoxic	Non-cytotoxic	79.49 ± 1.44	Inactive	Non-cytotoxic
15	3-Triazole	3,4-DiOMe	38.57 ± 1.48	Non-cytotoxic	Non-cytotoxic	3.91 ± 0.34	Inactive	Non-cytotoxic
16	3-Triazole	2,3-DiOMe	2.36 ± 0.14	4.26 ± 0.29	18.06 ± 1.07	0.53 ± 0.08	4.73	3.91
17	3-Triazole	2,3,4-TriOMe	6.13 ± 0.06	Non-cytotoxic	Non-cytotoxic	1.13 ± 0.18	7.47	Non-cytotoxic
18	4-Triazole	2,3,4-TriOMe	Non-cytotoxic	22.85 ± 0.51	Non-cytotoxic	12.33 ± 1.78	1.60	Non-cytotoxic
19	4-Triazole	3,4,5-TriOMe	Non-cytotoxic	Non-cytotoxic	Non-cytotoxic	6.58 ± 1.78	Inactive	Non-cytotoxic
Etoposide[c]			ND	30.16 ± 0.50	ND	0.051 ± 0.002	ND	ND
Doxorubicin[c]			0.83 ± 0.07	0.79 ± 0.08	0.44 ± 0.01	ND	ND	ND
Dihydroartemisinine[c]			ND	ND	ND	ND	0.0011	ND
Ellipticine[c]			ND	ND	ND	ND	ND	1.94

Non-cytotoxic = IC_{50} > 50 μg/mL.
Inactive = IC_{50} > 10 μg/mL.
Vero cell line = African green monkey kidney cell line.
ND, not determined.
[a] Cancer cell lines comprise the following: HuCCA-1 human cholangiocarcinoma cell line, HepG2 human hepatocellular carcinoma cell line, A549 human lung carcinoma cell line, MOLT-3 human lymphoblastic leukemia cell line.
[b] Antimalarial against *Plasmodium falciparum*.
[c] Etoposide, doxorubicin, ellipticine and dihydroartemisinine were used as reference drugs.

better cytotoxic activity than 7-coumaryls were shown to be in the following order **17** > **12**, **18** > **13** and **19** > **14**. Interestingly, HepG2 cells inhibitory action was observed for hybrids containing 2,3-dimethoxy (**10**, **11** and **16**) and 2,3,4-trimethoxy (**18**) on ring B. Such compounds (**10**, **11**, **16** and **18**) were shown to be more potent anticancer agents as compared to etoposide, the reference drug. Particularly, the most potent hybrid **16** (IC_{50} of 4.26 μM) displayed 7-fold stronger activity than the etoposide (IC_{50} = 30.16 μM). So far, the 2,3-dimethoxy derivatives **10** and **16** containing triazole ring at position 3 showed cytotoxicity against the Vero cell with IC_{50} of 35.03 and 3.91 μM, respectively. It should be noted that the hybrid **11** showed cytotoxicity in a broad spectrum of cancer cells (i.e., HuCCA-1, HepG2 and A549 cells) with IC_{50} values in the range of 4.81–8.18 μM without affecting normal cells. Molecular docking of the anticancer hybrids to their target proteins, tubulins have been described herein.

2.2.2. Antimalarial activity

Antimalarial activity of the hybrids (**9**–**19**) was examined against *Plasmodium falciparum* (K1, multidrug resistant strain) as shown in Table 1. The synthesized hybrids of 2,3-dimethoxy (**10** and **16**) and 2,3,4-trimethoxy (**12**, **17** and **18**) showed significant antimalarial activity with IC_{50} values in the range of 1.60–13.03 μM. At this point, it seemed reasonable that the presence of methoxy groups at *ortho*- and *para*-positions of chalcones (ring B) played crucial role for antimalarial activity. In addition, a series of 4-coumarinoxymethyl derivatives showed superior potency than the corresponding 7-coumarinoxymethyl analogs as seen for **16** > **10**, **17** > **12** and **18** > **13**. Notably, the 2,3,4-trimethoxy analog **18** was shown to be the most potent compound (IC_{50} = 1.60 μM) and was non-toxic to normal cells. Results from the molecular docking of antimalarial analogs are discussed hereafter.

2.3. Validation of docking protocol

Co-crystallized ligands, colchicine and *trans*-epoxysuccinyl-*L*-leucylamido-(4-guanidino)butane (E64), were re-docked to their target proteins, tubulin and falcipain-2, as to validate the docking protocol. Owing to limitations of the available docking software, covalent bonds between E64 and the falcipain-2 active site were disrupted and re-docked *via* non-covalent docking. Colchicine and E64 could be re-docked to their respective target proteins with a root mean squared deviation (RMSD) of 0.697 Å (Fig. 4A) and 1.157 Å (Fig. 4B), respectively.

2.3.1. Molecular docking of chalcone–triazole–coumarin derivatives to α- and β-tubulin complexes

As previously mentioned, the cytotoxic activity of chalcone is often associated with its ability to inhibit β-tubulin formation *via* binding of compounds to the colchicine binding site [5–7]. Molecular docking was performed to investigate the binding modalities of chalcone–triazole–coumarin derivatives against tubulin. Results suggested that all chalcone–triazole–coumarin analogs could snugly occupy the colchicine binding site of β-tubulin as shown in Fig. 4C. Binding energies for these compounds are in the range of −9.6 to −10.8 kcal/mol (Table 2). It was observed that all chalcone–triazole–coumarin derivatives afforded stronger binding energies than that of the colchicine found in the co-crystallized structure thereby suggesting promising inhibitory effect for this set of compounds. The observed tubulin binding energies for these compounds are in accordance with their cytotoxic activities, in which the more potent compounds as seen for the dimethoxy analogs (**9**–**11**, **15** and **16**) displayed lower binding energies (−10.5 to −10.8 kcal/mol) than the trimethoxy analogs (**12**–**14** and **17**–**19**) with the binding energies in the range of −9.6 to −10.3 kcal/mol. Particularly, the lowest cytotoxic activity of compound **14** showed the highest tubulin binding energy of −9.6 kcal/mol. Interestingly, docking poses of these compounds revealed that they could also occupy the GTP binding site of α-tubulin that is adjacent to the colchicine binding site of β-tubulin. These findings suggest that chalcone–triazole–coumarin derivatives could plausibly act as dual site inhibitors of α- and β-tubulin complexes. Molecular modeling analysis of the crystal structure revealed that the co-crystallized colchicine interacts with β-tubulin *via* the formation of hydrogen bonds involving a methoxy group to Cys241 and engaging in hydrophobic interactions with Leu255 and Ala316 (Fig. 4A). The GTP binds α-tubulin *via* the formation of hydrogen bonding network between the phosphate moiety to Ala12, Asp69,

Table 2
Binding energy of chalcone–triazole–coumarin derivatives (**9**–**19**).

Compounds	Binding energy (kcal/mol)[a]	
	Tubulin	Falcipain-2
9	−10.8	ND
10	−10.6	−8.6
11	−10.5	ND
12	−10.2	−8.9
13	−9.8	ND
14	−9.6	ND
15	−10.6	ND
16	−10.7	−8.3
17	−10.3	−8.1
18	−10.1	−8.4
19	−10.0	ND
Colchicine	−9.4	ND
E64[b]	ND	−7.3

[a] *ND*, not determined.
[b] E64 was covalently bound to falcipain-2. Binding energy was obtained from non-covalent docking.

Ser140, Thr145, Ser178 and Glu183 while the guanine ring forms hydrogen bonds with Asn206 and Asn288 as well as π–π stacking with Tyr224. Moreover, hydrophobic interaction between Ala12 and Tyr224 of α-tubulin with GTP were also observed. These aforementioned residues could be the essential site for ligand binding as to inhibit microtubule formation.

Compound **11**, which provided cytotoxicity against a broad spectrum of cancer cells (i.e., HuCCA-1, HepG2 and A549 cells) without affecting normal cells, could interact with both colchicine and GTP binding sites of β- and α-tubulins, respectively (Fig. 5A). The coumarin moiety of the compound could occupy the hydrophobic pocket as defined by Leu248, Ala316 and Ala354 residues of β-tubulin, which are located inside the colchicine binding site. In addition, ring B of chalcone moiety of the compound could form hydrophobic interaction with Ala12 and Tyr224 together with π–π interaction with Tyr224 of α-tubulin, which constitutes the GTP binding pocket. The less potency of trimethoxy analogs (**13**, **14**, **18** and **19**) compared to the 2,3-dimethoxy analog (**11**) may be due to the steric reason in this hydrophobic area. In addition, such interaction was strengthened by hydrogen bonding as afforded by the N atom at position 2 of triazole ring to Asn101 of α-tubulin and π–cation interaction of chalcone ring A to the positively-charged side chain of Lys254 from β-tubulin. These finding suggested that the cytotoxicity of chalcone–triazole–coumarin derivatives could be possibly due to their dual inhibition of α- and β-tubulins.

2.3.2. *Molecular docking of chalcone–coumarin derivatives to falcipain-2*

Many chalcone derivatives have been revealed to inhibit malarial cysteine protease [10–12], the enzyme plays an essential role in the degradation of host hemoglobin into small peptides as nutrients occurring within the acidic food vacuole of the parasite. Accordingly, molecular docking was performed against the cysteine protease-like falcipain-2 using selected compounds (i.e., **10**, **12**, **16**, **17** and **18**) that have been shown to exert antimalarial activity. The crystal structure of falcipain-2 was co-crystallized with inhibitor E64, which was covalently-bonded to the enzyme as to block substrates from reaching the catalytic triad as defined by Gln36, Cys42 and His174 residues [41]. Docking results suggested that all selected compounds could bind the active site of falcipain-2 (Fig. 4D) with binding energies in the range of −8.1 to −8.9 kcal/mol (Table 2). Unfortunately, due to the limitation of available docking software in performing covalent docking, therefore the

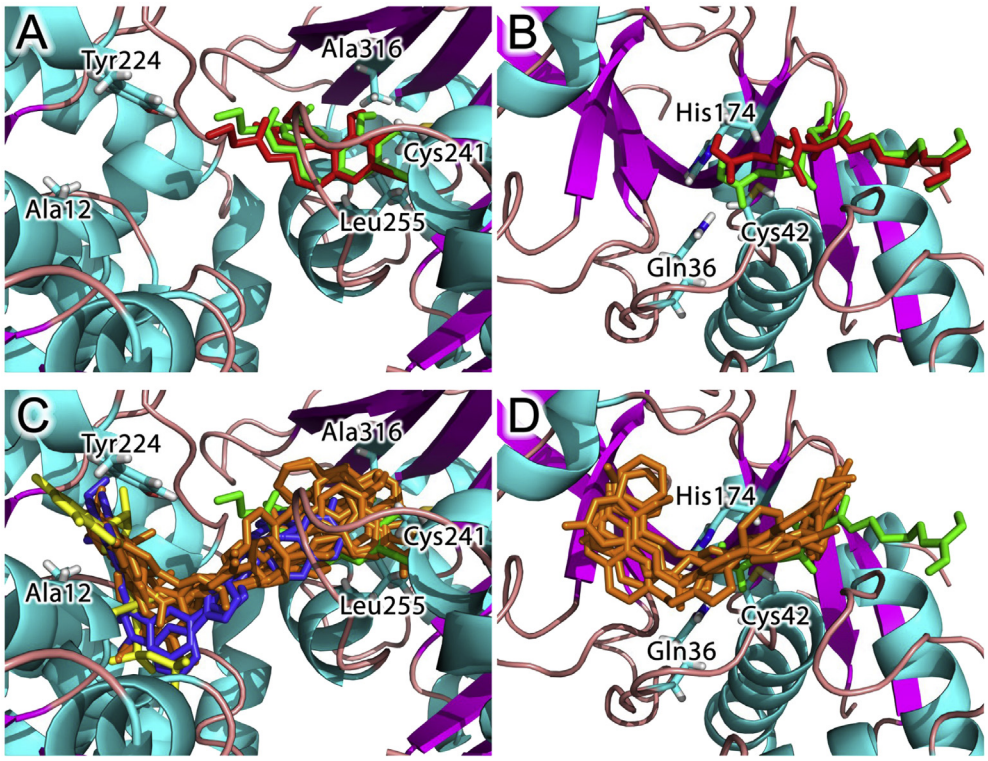

Fig. 4. Molecular docking of chalcone–triazole–coumarin ligands to tubulin. Re-docking poses of colchicine to tubulin (A) and E64 to falcipain-2 (B) are shown with original ligand structures colored in green while re-docking poses colored in red. Docking poses of chalcone–triazole–coumarin ligands to tubulin (C) are shown with colchicine colored in green, GTP colored in yellow, ligands colored in orange and blue. Docking poses of chalcone–triazole–coumarin ligands to falcipain-2 (D) are shown with E64 colored in green and ligands colored in orange. (For interpretation of the references to color in this figure legend, the reader is referred to the web version of this article.)

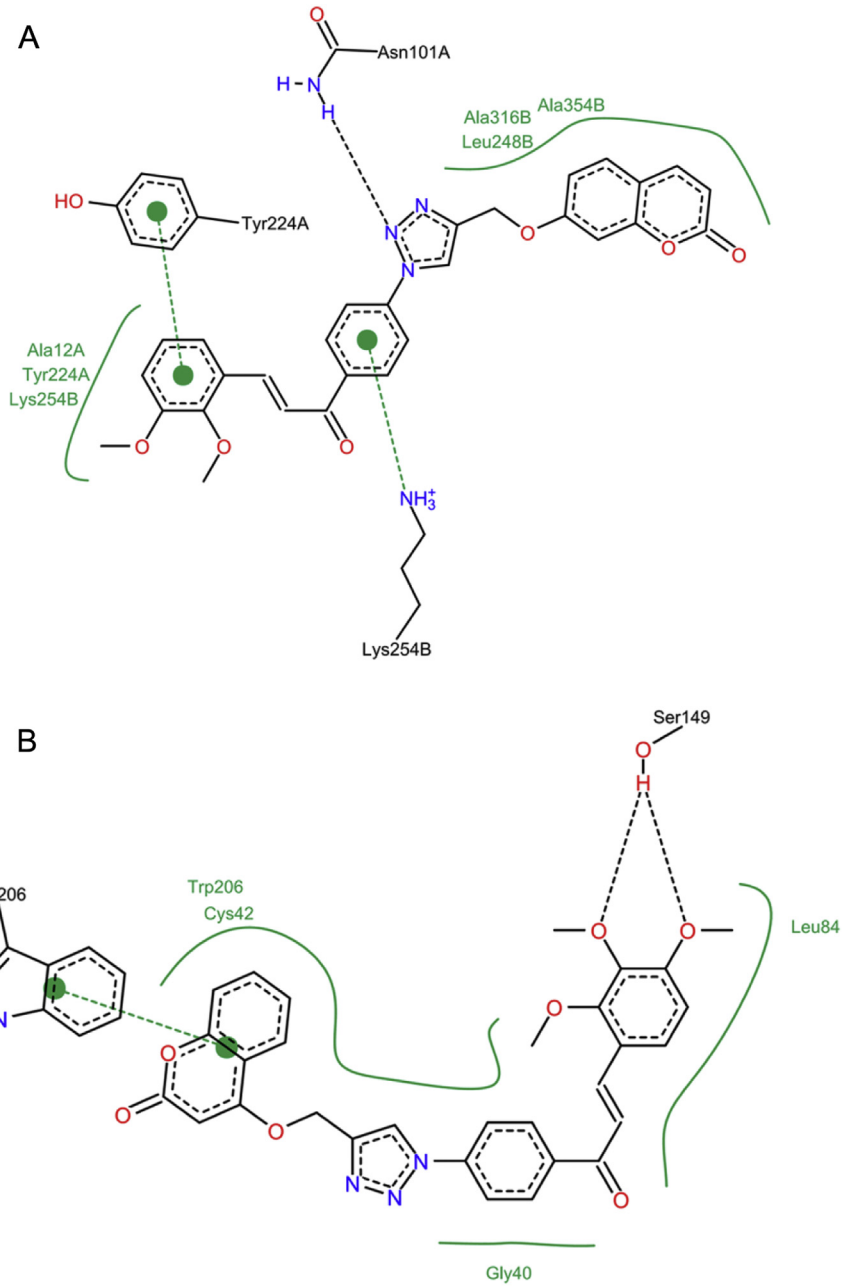

Fig. 5. Two-dimensional schematics of the protein-ligand interaction of compound **11** to tubulin (A) and compound **18** to falcipain-2 (B). The amino acid residues such as Ala12A, A is denoted as α-tubulin; and Ala316B, B is denoted as β-tubulin.

binding energy of E64 was obtained by disrupting the covalent bond and re-docked non-covalently. Owing to these inherent differences in the binding mechanism, thus it cannot be assumed that the chalcone–triazole–coumarins could possess higher potency than E64 by judging from their binding energies. Compound **18**, which had the highest antimalarial activity, could bind the active site of falcipain-2 *via* the interaction scheme shown in Fig. 5B. As such, the coumarin moiety of the compound could occupy the binding site of falcipain-2 *via* hydrophobic interaction with Cys42 and Trp206 residues together with the formation of $\pi-\pi$ stacking with Trp206. Such interaction afforded strong stability because ring A and ring B of chalcone moiety formed hydrophobic interaction with Gly40 and Leu84, respectively. Moreover, 3,4-dimethoxy substituents of chalcone ring B provided hydrogen bonding with Ser149 thereby resulting in tight binding of compound **18** to the falcipain-2 active site. The docking results suggested that the antimalarial activity of the chalcone–triazole–coumarin derivatives might be due to their inhibitions of falcipain-2.

Furthermore, metabolic pathways in intracellular parasites (i.e., *P. falciparum*) and cancer cells are more sensitive to oxidative stress than normal cells [42]. It could be presumably explained that dimethoxychalcone moieties might be metabolized to catechols, then to phenoxy radicals and ultimately to superoxide anions, which are toxic to the cells [5].

3. Conclusions

Eleven conjugated molecules (**9**–**19**) derived from chalcones and coumarins linked by 1,2,3-triazole ring have been successfully synthesized *via* the Click reaction. Cytotoxic activity testing

revealed that most of the hybrids displayed cytotoxicity against MOLT-3 cell line. In particular, the chalcone–coumarin **16** was the most potent cytotoxic agent (IC_{50} = 0.53 μM). Compounds **10**, **11**, **16** and **18** displayed higher cytotoxic potency against HepG2 cells than the control drug, etoposide. The hybrid **16** was shown to be the most potent one (IC_{50} = 4.26 μM), but unfortunately it was toxic toward non-cancerous (Vero) cells. Significantly, the analog **11** displayed the second most potent activity (HepG2) with IC_{50} value of 8.18 μM and non-toxic to Vero cells. Importantly, antimalarial activity results concluded that the conjugate **18** exhibited the most potent activity (IC_{50} = 1.60 μM) without affecting non-cancerous cells. Docking results suggested that the cytotoxic and antimalarial activities of the hybrids might be due to their inhibition of tubulin and falcipain-2, respectively. This study provides novel chalcone–coumarin hybrids as potential lead molecules for further structural optimization as anticancer and antimalarial agents.

4. Experimental

4.1. Chemistry

Column chromatography was carried out using silica gel 60 (70–230 mesh ASTM). Analytical thin-layer chromatography (TLC) was performed on silica gel 60 F_{254} aluminum sheets. ^{1}H and ^{13}C NMR spectra were recorded on a Bruker AVANCE 300 NMR spectrometer (operating at 300 MHz for ^{1}H and 75 MHz for ^{13}C). FTIR spectra were obtained using a universal attenuated total reflectance attached on a Perkin–Elmer Spectrum One spectrometer. High resolution mass spectra (HRMS) were recorded on a Bruker Daltonics (microTOF). Melting points were determined using a Griffin melting point apparatus and were uncorrected.

4.2. General procedure for the synthesis of aminochalcones (**6**)

To a stirred solution of benzaldehyde **4** (5 mmol) and aminoacetophenone **5** (5 mmol) in ethanol (15 mL) at 5 °C, then 40% KOH (10 mL) was added dropwise, and stirred at room temperature overnight. The reaction mixture was neutralized with 2 M HCl, and then extracted with ethyl acetate (3 × 30 mL). The combined organic phases were washed with water (25 mL), dried over anhydrous sodium sulfate and evaporated to dryness. The crude product was purified using silica gel column chromatography and eluted with 12% acetone–hexane.

4.2.1. (*E*)-1-(3-aminophenyl)-3-(3,4-dimethoxyphenyl)prop-2-en-1-one (**6a**)

Yellow solid. 57%. mp 68–69 °C. IR (UATR) cm^{-1}: 3448, 3362, 3225, 1652, 1621, 1574, 1508. ^{1}H NMR (300 MHz, $CDCl_3$) δ 2.80 (br s, 2H, NH_2), 3.95, 3.96 (2s, 6H, 2 × OCH_3), 6.91 (d, *J* = 8.3 Hz, 1H, C5′-Ar*H*), 6.95 (d, *J* = 7.7 Hz, 1H, C4-Ar*H*), 7.16 (d, *J* = 1.4 Hz, 1H, C2′-Ar*H*), 7.23 (d, *J* = 8.3 Hz, 1H, C6′-Ar*H*), 7.30 (t, *J* = 7.2 Hz, 1H, C5-Ar*H*), 7.35 (d, *J* = 15.4 Hz, 1H, CH=C*H*CO), 7.38 (s, 1H, C2-Ar*H*), 7.42 (d, *J* = 7.5 Hz, 1H, C6-Ar*H*), 7.75 (d, *J* = 15.6 Hz, 1H, C*H*=CHCO). ^{13}C NMR (75 MHz, $CDCl_3$) δ 56.0, 110.1, 111.1, 114.8, 119.2, 119.6, 120.3, 123.1, 127.9, 129.4, 139.6, 144.8, 146.0, 149.2, 151.4, 190.8. HRMS-TOF: *m*/*z* [M+Na]$^+$ 306.1102 (Calcd for $C_{17}H_{17}NNaO_3$: 306.1101).

4.2.2. (*E*)-1-(3-aminophenyl)-3-(2,3-dimethoxyphenyl)prop-2-en-1-one (**6b**)

Yellow oil. 41%. IR (UATR) cm^{-1}: 3462, 3367, 3229, 1656, 1623, 1575, 1477. ^{1}H NMR (300 MHz, $CDCl_3$) δ 2.90 (br s, 2H, NH_2), 3.86, 3.87 (2s, 6H, 2 × OCH_3), 6.87 (d, *J* = 7.9 Hz, 1H, C4-Ar*H*), 6.94 (d, *J* = 8.1 Hz, 1H, C4′-Ar*H*), 7.07 (t, *J* = 8.0 Hz, 1H, C5′-Ar*H*), 7.21–7.28 (m, 2H, C5-Ar*H*, C6′-Ar*H*), 7.31 (s, 1H, C2-Ar*H*), 7.37 (d, *J* = 7.6 Hz, 1H, C6-Ar*H*), 7.53 (d, *J* = 15.9 Hz, 1H, CH=C*H*CO), 8.05 (d, *J* = 15.9 Hz, 1H, C*H*=CHCO). ^{13}C NMR (75 MHz, $CDCl_3$) δ 55.9, 61.3, 114.1, 114.6, 119.0, 119.4, 119.6, 123.9, 124.2, 129.2, 129.4, 139.3, 139.4, 146.7, 149.0, 153.2, 191.0. HRMS-TOF: *m*/*z* HRMS-TOF: *m*/*z* [M+Na]$^+$ 306.1113 (Calcd for $C_{17}H_{17}NNaO_3$: 306.1101).

4.2.3. (*E*)-1-(4-aminophenyl)-3-(2,3-dimethoxyphenyl)prop-2-en-1-one (**6c**)

Yellow solid. 65%. mp 133–134 °C (135.6–136.8 °C [43]). IR (UATR) cm^{-1}: 3453, 3351, 3228, 1623, 1602, 1579, 1478. ^{1}H NMR (300 MHz, $CDCl_3$) δ 3.90, 3.91 (2s, 6H, 2 × OCH_3), 4.17 (br s, 2H, NH_2), 6.72 (d, *J* = 8.7 Hz, 2H, C3-Ar*H*, C5-Ar*H*), 6.97 (d, *J* = 8.0 Hz, 1H, C-4′-Ar*H*), 7.10 (t, *J* = 8.0 Hz, 1H, C-5′-Ar*H*), 7.29 (d, *J* = 8.0 Hz, 1H, C-6′-Ar*H*), 7.62 (d, *J* = 15.8 Hz, 1H, CH=C*H*CO), 7.95 (d, *J* = 8.6 Hz, 2H, C2-Ar*H*, C6-Ar*H*), 8.07 (d, *J* = 15.8 Hz, 1H, C*H*=CHCO). ^{13}C NMR (75 MHz, $CDCl_3$) δ 55.9, 61.3, 113.8, 113.9, 119.6, 123.8, 124.1, 128.7, 129.6, 131.1, 138.0, 148.8, 151.0, 153.2, 188.5. HRMS-TOF: *m*/*z* [M+H]$^+$ 284.1285 (Calcd for $C_{17}H_{18}NO_3$: 284.1281).

4.2.4. (*E*)-1-(3-aminophenyl)-3-(2,3,4-trimethoxyphenyl)prop-2-en-1-one (**6d**)

Yellow solid. 62%. mp 94–95 °C. IR (UATR) cm^{-1}: 3458, 3364, 3233, 1653, 1627, 1577, 1494. ^{1}H NMR (300 MHz, $CDCl_3$) δ 3.85 (br s, 2H, NH_2), 3.91, 3.93, 3.96 (3s, 9H, 3 × OCH_3), 6.74 (d, *J* = 8.8 Hz, 1H, C5′-Ar*H*), 6.90 (dd, *J* = 8.0, 1.9 Hz, 1H, C4-Ar*H*), 7.29 (t, *J* = 7.8 Hz, 1H, C5-Ar*H*), 7.34 (t, *J* = 1.9 Hz, 1H, C2-Ar*H*), 7.40 (d, *J* = 8.7 Hz, 2H, C6-Ar*H*, C6′-Ar*H*), 7.53 (d, *J* = 15.8 Hz, 1H, CH=C*H*CO), 7.99 (d, *J* = 15.8 Hz, 1H, C*H*=CHCO). ^{13}C NMR (75 MHz, $CDCl_3$) δ 56.1, 60.9, 61.4, 107.6, 114.5, 118.8, 119.2, 121.7, 122.1, 123.8, 129.4, 139.7, 139.8, 142.5, 146.8, 153.8, 155.7, 191.1. HRMS-TOF: *m*/*z* [M+H]$^+$ 314.1390 (Calcd for $C_{18}H_{20}NO_4$: 314.1387).

4.2.5. (*E*)-1-(4-aminophenyl)-3-(2,3,4-trimethoxyphenyl)prop-2-en-1-one (**6e**)

Yellow solid. 80%. mp 125–126 °C. IR (UATR) cm^{-1}: 3458, 3343, 3234, 1633, 1595, 1580, 1494. ^{1}H NMR (300 MHz, $CDCl_3$) δ 3.87, 3.88, 3.91 (3s, 9H, 3 × OCH_3), 4.15 (br s, 2H, NH_2), 6.67 (d, *J* = 8.7 Hz, 2H, C3-Ar*H*, C5-Ar*H*), 6.69 (d, *J* = 8.8 Hz, 1H, C5′-Ar*H*), 7.35 (d, *J* = 8.8 Hz, 1H, C6′-Ar*H*), 7.55 (d, *J* = 15.7 Hz, 1H, CH=C*H*CO), 7.90 (d, *J* = 8.7 Hz, 2H, C2-Ar*H*, C6-Ar*H*), 7.93 (d, *J* = 15.7 Hz, 1H, C*H*=CHCO). ^{13}C NMR (75 MHz, $CDCl_3$) δ 56.1, 60.9, 61.4, 107.6, 113.9, 121.5, 122.5, 123.7, 128.9, 131.0, 138.4, 142.5, 150.9, 153.6, 155.4, 188.6. HRMS-TOF: *m*/*z* [M+H]$^+$ 314.1395 (Calcd for $C_{18}H_{20}NO_4$: 314.1387).

4.2.6. (*E*)-1-(4-aminophenyl)-3-(3,4,5-trimethoxyphenyl)prop-2-en-1-one (**6f**)

Yellow solid. 72%. mp 156–157 °C (160 °C [44]). IR (UATR) cm^{-1}: 3457, 3361, 3234, 1628, 1604, 1584, 1504. ^{1}H NMR (300 MHz, $CDCl_3$) δ 3.91, 3.94 (2s, 9H, 3 × OCH_3), 4.20 (br s, 2H, NH_2), 6.72 (d, *J* = 8.5 Hz, 2H, C3-Ar*H*, C5-Ar*H*), 6.87 (s, 2H, C2′-Ar*H*, C6′-Ar*H*), 7.43 (d, *J* = 15.5 Hz, 1H, CH=C*H*CO), 7.72 (d, *J* = 15.5 Hz, 1H, C*H*=CHCO),7.95 (d, *J* = 8.5 Hz, 2H, C2-Ar*H*, C6-Ar*H*). ^{13}C NMR (75 MHz, $CDCl_3$) δ 56.2, 61.0, 105.5, 113.9, 121.4, 128.6, 130.9, 131.1, 140.1, 143.3, 151.1, 153.5, 188.0. HRMS-TOF: *m*/*z* [M+H]$^+$ 314.1390 (Calcd for $C_{18}H_{20}NO_4$: 314.1387).

4.3. General procedure for the synthesis of azidochalcones (**7**)

To a cold solution of aminochalcone **6** (3 mmol) in HCl:CH_3COOH (3:3 mL) at 0 °C, a solution of sodium nitrite (9 mmol) in water (5 mL) was added. The stirred reaction mixture was maintained for 15 min and then added dropwise a solution of sodium azide (9 mmol) in water (5 mL). The reaction mixture was allowed to stir at room temperature for 0.5 h, then the precipitate was filtered, washed with cold water and recrystallized from methanol.

*4.3.1. (E)-1-(3-azidophenyl)-3-(3,4-dimethoxyphenyl)prop-2-en-1-one (**7a**)*

Yellow solid. 77%. mp 75–76 °C. IR (UATR) cm^{-1}: 2105, 1660, 1576, 1511. ^1H NMR (300 MHz, $CDCl_3$) δ 3.92, 3.94 (2s, 6H, 2 × OCH_3), 6.89 (d, J = 8.3 Hz, 1H, C5′-Ar*H*), 7.13 (d, J = 1.9 Hz, 1H, C2′-Ar*H*), 7.19–7.24 (m, 2H, C4-Ar*H*, C6′-Ar*H*), 7.31 (d, J = 15.6 Hz, 1H, CH=C*H*CO), 7.47 (t, J = 7.9 Hz, 1H, C5-Ar*H*), 7.64 (d, J = 1.9 Hz, 1H, C2-Ar*H*), 7.74 (d, J = 7.9 Hz, 1H, C6-Ar*H*), 7.75 (d, J = 15.6 Hz, 1H, C*H*=CHCO). ^{13}C NMR (75 MHz, $CDCl_3$) δ 56.0, 110.1, 111.1, 118.8, 119.6, 122.9, 123.4, 124.8, 127.6, 130.0, 140.2, 140.9, 145.8, 149.3, 151.7, 189.6. HRMS-TOF: m/z $[M+H]^+$ 310.1200 (Calcd for $C_{17}H_{16}N_3O_3$: 310.1186).

*4.3.2. (E)-1-(3-azidophenyl)-3-(2,3-dimethoxyphenyl)prop-2-en-1-one (**7b**)*

Yellow solid. 78%. mp 73–74 °C. IR (UATR) cm^{-1}: 2109, 1663, 1577, 1479. ^1H NMR (300 MHz, $CDCl_3$) δ 3.87, 3.88 (2s, 6H, 2 × OCH_3), 6.97 (dd, J = 8.1, 1.3 Hz, 1H, C4′-Ar*H*), 7.09 (t, J = 7.9 Hz, 1H, C5′-Ar*H*), 7.18–7.28 (m, 2H, C4-Ar*H*, C6′-Ar*H*), 7.45 (t, J = 8.0 Hz, 1H, C5-Ar*H*), 7.48 (d, J = 15.8 Hz, 1H, CH=C*H*CO), 7.65 (t, J = 1.8 Hz, 1H, C2-Ar*H*), 7.75 (d, J = 7.7 Hz, 1H, C6-Ar*H*), 8.09 (d, J = 15.8 Hz, 1H, C*H*=CHCO). ^{13}C NMR (75 MHz, $CDCl_3$) δ 55.9, 61.3, 114.5, 118.9, 119.7, 123.1, 123.2, 124.2, 125.0, 128.9, 130.0, 140.0, 140.5, 140.9, 153.3, 189.9. HRMS-TOF: m/z $[M+H]^+$ 310.1191 (Calcd for $C_{17}H_{16}N_3O_3$: 310.1186).

*4.3.3. (E)-1-(4-azidophenyl)-3-(2,3-dimethoxyphenyl)prop-2-en-1-one (**7c**)*

Orange-yellow solid. 69%. mp 82–83 °C. IR (UATR) cm^{-1}: 2122, 1660, 1601, 1577, 1479. ^1H NMR (300 MHz, $CDCl_3$) δ 3.91 (s, 6H, 2 × OCH_3), 7.00 (dd, J = 8.0, 1.3 Hz, 1H, C4′-Ar*H*), 7.12 (t, J = 8.0 Hz, 1H, C5′-Ar*H*), 7.15 (d, J = 8.7 Hz, 2H, C3-Ar*H*, C5-Ar*H*), 7.29 (d, J = 8.0 Hz, 1H, C6′-Ar*H*), 7.59 (d, J = 15.9 Hz, 1H, CH=C*H*CO), 8.07 (d, J = 8.7 Hz, 2H, C2-Ar*H*, C6-Ar*H*), 8.12 (d, J = 15.9 Hz, 1H, C*H*=CHCO). ^{13}C NMR (75 MHz, $CDCl_3$) δ 55.9, 61.3, 114.3, 119.0, 119.7, 123.2, 124.2, 129.1, 130.5, 135.0, 139.8, 144.6, 149.0, 153.3, 189.1. HRMS-TOF: m/z $[M+H]^+$ 310.1195 (Calcd for $C_{17}H_{16}N_3O_3$: 310.1186).

*4.3.4. (E)-1-(3-azidophenyl)-3-(2,3,4-trimethoxyphenyl)prop-2-en-1-one (**7d**)*

Yellow solid. 93%. mp 65–66 °C. IR (UATR) cm^{-1}: 2107, 1660, 1576, 1495. ^1H NMR (300 MHz, $CDCl_3$) δ 3.91, 3.94, 3.98 (3s, 9H, 3 × OCH_3), 6.75 (d, J = 8.8 Hz, 1H, C5′-Ar*H*), 7.23 (dd, J = 7.8, 1.8 Hz, 1H, C4-Ar*H*), 7.41 (d, J = 8.8 Hz, 1H, C6′-Ar*H*), 7.50 (t, J = 7.8 Hz, 1H, C5-Ar*H*), 7.52 (d, J = 15.8 Hz, 1H, CH=C*H*CO), 7.68 (t, J = 1.8 Hz, 1H, C2-Ar*H*), 7.78 (d, J = 7.8 Hz, 1H, C6-Ar*H*), 8.03 (d, J = 15.8 Hz, 1H, C*H*=CHCO). ^{13}C NMR (75 MHz, $CDCl_3$) δ 56.1, 60.9, 61.4, 107.6, 118.8, 120.9, 121.8, 122.9, 124.1, 124.9, 129.9, 140.3, 140.8, 141.0, 142.5, 154.0, 156.0, 189.9. HRMS-TOF: m/z $[M+H]^+$ 340.1299 (Calcd for $C_{18}H_{18}N_3O_4$: 340.1292).

*4.3.5. (E)-1-(4-azidophenyl)-3-(2,3,4-trimethoxyphenyl)prop-2-en-1-one (**7e**)*

Yellow solid. 93%. mp 115–116 °C. IR (UATR) cm^{-1}: 2126, 1654, 1598, 1584, 1494. ^1H NMR (300 MHz, $CDCl_3$) δ 3.92, 3.94, 3.97 (3s, 6H, 3 × OCH_3), 6.75 (d, J = 8.8 Hz, 1H, C5′-Ar*H*), 7.15 (d, J = 8.5 Hz, 2H, C3-Ar*H*, C5-Ar*H*), 7.41 (d, J = 8.8 Hz, 1H, C6′-Ar*H*), 7.56 (d, J = 15.7 Hz, 1H, CH=C*H*CO), 8.02 (d, J = 15.7 Hz, 1H, C*H*=CHCO), 8.06 (d, J = 8.5 Hz, 2H, C2-Ar*H*, C6-Ar*H*). ^{13}C NMR (75 MHz, $CDCl_3$) δ 56.1, 60.9, 61.4, 107.6, 119.0, 120.9, 122.0, 124.0, 130.4, 135.3, 140.3, 142.6, 144.4, 153.9, 155.9, 189.1. HRMS-TOF: m/z HRMS-TOF: m/z $[M+H]^+$ 340.1283 (Calcd for $C_{18}H_{18}N_3O_4$: 340.1292).

*4.3.6. (E)-1-(4-azidophenyl)-3-(3,4,5-trimethoxyphenyl)prop-2-en-1-one (**7f**)*

Yellow solid. 90%. mp 70–71 °C. IR (UATR) cm^{-1}: 2122, 1658, 1599, 1579, 1502. ^1H NMR (300 MHz, $CDCl_3$) δ 3.92, 3.94 (2s, 6H, 3 × OCH_3), 6.88 (s, 2H, C2′-Ar*H*, C6′-Ar*H*), 7.15 (d, J = 8.1 Hz, 2H, C3-Ar*H*, C5-Ar*H*), 7.39 (d, J = 15.5 Hz, 1H, CH=C*H*CO), 7.75 (d, J = 15.5 Hz, 1H, C*H*=CHCO), 8.05 (d, J = 8.1 Hz, 2H, C2-Ar*H*, C6-Ar*H*). ^{13}C NMR (75 MHz, $CDCl_3$) δ 56.3, 61.0, 105.8, 119.1, 120.9, 130.3, 130.5, 134.9, 140.6, 144.7, 145.1, 153.5, 188.7. HRMS-TOF: m/z HRMS-TOF: m/z $[M+H]^+$ 340.1288 (Calcd for $C_{18}H_{18}N_3O_4$: 340.1292).

*4.4. General procedure for the synthesis of propynyloxy derivatives (**8a**–**b**)*

A propargyl bromide (2.4 mmol) was added to a suspension of an appropriate coumarin (2 mmol) and potassium carbonate (4 mmol) in acetone (15 mL). The suspension was heated under reflux for 2 h. The reaction was allowed to cool and then concentrated under reduced pressure. Water (30 mL) was added and extracted with EtOAc (3 × 30 mL). The organic extracts were combined and washed with water (20 mL) and brine (20 mL). The organic layer was dried over anhydrous sodium sulfate, filtered and concentrated *in vacuo*. The crude product was purified by column chromatography.

^1H NMR spectra of 7-(propynyloxy)-2*H*-chromen-2-one (**8a**) [45] and 4-(propynyloxy)-2*H*-chromen-2-one (**8b**) [46] were consistent with those reported in the literatures.

*4.5. General procedure for the synthesis of chalcone–coumarin hybrids (**9**–**19**)*

To a stirred solution of azidochalcone **7** (0.2 mmol) and alkyne **8** (0.22 mmol) in *t*-BuOH:H_2O (3:3 mL), $CuSO_4 \cdot 5H_2O$ (0.22 mmol) and sodium ascorbate (0.5 mmol) was added. The reaction mixture was stirred at room temperature for 2 h and then concentrated under reduced pressure. The residue was added water (10 mL) and extracted with dichloromethane (3 × 20 mL). The combined organic phases were washed with water (20 mL), dried over anhydrous sodium sulfate and evaporated to dryness. The crude product was purified using silica gel column chromatography and eluted with methanol:dichloromethane (1:50).

*4.5.1. (E)-7-((1-(3-(3-(3,4-dimethoxyphenyl)acryloyl)phenyl)-1H-1,2,3-triazol-4-yl)methoxy)-2H-chromen-2-one (**9**)*

Starting from azidochalcone **7a** and alkyne **8a**. Yellow solid. 65%. mp 132–133 °C. IR (UATR) cm^{-1}: 1723, 1660, 1611, 1576, 1509, 1464. ^1H NMR (300 MHz, $CDCl_3$) δ 3.92, 3.94 (2s, 6H, 2 × OCH_3), 5.35 (s, 2H, CH_2O), 6.25 (d, J = 9.5 Hz, 1H, C3), 6.89 (d, J = 8.3 Hz, 1H, C5″-Ar*H*), 6.92–6.98 (m, 2H, C6 and C8), 7.16 (s, 1H, C2″-Ar*H*), 7.25 (d, J = 8.3 Hz, 1H, C6″-Ar*H*), 7.38 (d, J = 15.6 Hz, 1H, CH=C*H*CO), 7.39 (d, J = 8.9 Hz, 2H, C5), 7.62 (d, J = 9.5 Hz, 1H, C4), 7.68 (t, J = 7.9 Hz, 1H, C5′-Ar*H*), 7.82 (d, J = 15.6 Hz, 1H, C*H*=CHCO), 8.01 (d, J = 8.0 Hz, 1H, C4′-Ar*H*), 8.07 (d, J = 7.7 Hz, 1H, C6′-Ar*H*), 8.20 (s, 1H, C*H*N), 8.32 (s, 1H, C2′-Ar*H*). ^{13}C NMR (75 MHz, $CDCl_3$) δ 56.1, 62.3, 102.2, 110.3, 111.2, 112.7, 113.2, 113.6, 119.0, 120.1, 121.3, 123.6, 124.3, 127.5, 128.7, 129.0, 130.2, 137.3, 140.2, 143.2, 144.1, 146.5, 149.4, 151.9, 155.8, 161.0, 161.2, 188.9. HRMS-TOF: m/z $[M+Na]^+$ 532.1464 (Calcd for $C_{29}H_{23}N_3NaO_6$: 532.1479).

*4.5.2. (E)-7-((1-(3-(3-(2,3-dimethoxyphenyl)acryloyl)phenyl)-1H-1,2,3-triazol-4-yl)methoxy)-2H-chromen-2-one (**10**)*

Starting from azidochalcone **7b** and alkyne **8a**. Pale yellow solid. 61%. mp 131–132 °C. IR (UATR) cm^{-1}: 1726, 1663, 1610, 1587, 1576, 1506, 1478. ^1H NMR (300 MHz, $CDCl_3$) δ 3.88 (s, 6H, 2 × OCH_3), 5.35 (s, 2H, CH_2O), 6.26 (d, J = 9.5 Hz, 1H, C3), 6.93–7.00 (m, 2H, C6, C8

and C4″-Ar*H*), 7.10 (t, *J* = 7.9 Hz, 1H, C5″-Ar*H*), 7.28 (dd, *J* = 7.9, 1.2 Hz, 1H, C6″-Ar*H*), 7.39 (d, *J* = 9.3 Hz, 1H, C5), 7.55–7.71 (m, 3H, C4, C5′-Ar*H* and CH=C*H*CO), 8.05–8.14 (m, 2H, C4′-Ar*H* and C6′-Ar*H*), 8.18 (d, *J* = 15.9 Hz, 1H, C*H*=CHCO), 8.25 (s, 1H, C*H*N), 8.36 (t, *J* = 1.8 Hz, 1H, C2′-Ar*H*). ^{13}C NMR (75 MHz, $CDCl_3$) δ 56.0, 61.4, 62.3, 102.2, 112.7, 113.2, 113.6, 114.7, 119.7, 120.2, 121.2, 122.8, 124.3, 124.4, 128.7, 128.8, 129.0, 130.3, 137.3, 139.9, 141.2, 143.2, 144.1, 149.2, 153.3, 155.8, 161.0, 161.2, 189.3. HRMS-TOF: *m*/*z* $[M+Na]^+$ 532.1488 (Calcd for $C_{29}H_{23}N_3NaO_6$: 532.1479).

4.5.3. (E)-7-((1-(4-(3-(2,3-dimethoxyphenyl)acryloyl)phenyl)-1H-1,2,3-triazol-4-yl)methoxy)-2H-chromen-2-one (**11**)

Starting from azidochalcone **7c** and alkyne **8a**. White solid. 80%. mp 228–229 °C. IR (UATR) cm^{-1}: 1741, 1659, 1621, 1608, 1577, 1479. ^{1}H NMR (300 MHz, DMSO-d_6) δ 3.82, 3.85 (2s, 6H, 2 × OCH_3), 5.40 (s, 2H, CH_2O), 6.32 (d, *J* = 9.5 Hz, 1H, C3), 7.06 (dd, *J* = 8.6, 2.4 Hz, 1H, C6), 7.15–7.24 (m, 3H, C8 and C4″-Ar*H*, C5″-Ar*H*), 7.67 (d, *J* = 8.8 Hz, 2H, C5 and C6″-Ar*H*), 7.93–8.08 (m, 3H, C4 and C*H*=C*H*CO), 8.15 (d, *J* = 8.7 Hz, 2H, C3′-Ar*H* and C5′-Ar*H*), 8.37 (d, *J* = 8.7 Hz, 2H, C2′-Ar*H* and C6′-Ar*H*), 9.17 (s, 1H, C*H*N). ^{13}C NMR (75 MHz, DMSO-d_6) δ 56.3, 61.5, 62.1, 102.1, 113.2, 113.3, 113.4, 115.8, 119.7, 120.5, 123.1, 123.8, 124.8, 128.6, 130.1, 130.9, 137.8, 139.0, 139.9, 144.0, 144.7, 148.9, 153.3, 155.8, 160.7, 161.5, 188.6. HRMS-TOF: *m*/*z* $[M+Na]^+$ 532.1480 (Calcd for $C_{29}H_{23}N_3NaO_6$: 532.1479).

4.5.4. (E)-7-((1-(3-(3-(2,3,4-trimethoxyphenyl)acryloyl)phenyl)-1H-1,2,3-triazol-4-yl)methoxy)-2H-chromen-2-one (**12**)

Starting from azidochalcone **7d** and alkyne **8a**. Yellow solid. 74%. mp 120–121 °C. IR (UATR) cm^{-1}: 1725, 1657, 1611, 1578, 1494. ^{1}H NMR (300 MHz, $CDCl_3$) δ 3.92, 3.95, 3.99 (3s, 9H, 3 × OCH_3), 5.40 (s, 2H, CH_2O), 6.30 (d, *J* = 9.5 Hz, 1H, C3), 6.76 (d, *J* = 8.8 Hz, 1H, C5″-Ar*H*), 6.97–7.03 (m, 2H, C6 and C8), 7.41–7.47 (m, 2H, C5 and C6″-Ar*H*), 7.58 (d, *J* = 15.8 Hz, 1H, CH=C*H*CO), 7.67 (d, *J* = 9.3 Hz, 2H, C4), 7.71 (t, *J* = 7.9 Hz, 1H, C5′-Ar*H*), 8.02–8.10 (m, 2H, C4′-Ar*H* and C6′-Ar*H*), 8.09 (d, *J* = 15.8 Hz, 1H, C*H*=CHCO), 8.23 (s, 1H, C*H*N), 8.36 (t, *J* = 1.7 Hz, 1H, C2′-Ar*H*). ^{13}C NMR (75 MHz, $CDCl_3$) δ 56.1, 61.0, 61.5, 62.3, 102.2, 107.7, 112.7, 113.2, 113.6, 120.1, 120.4, 121.2, 121.6, 124.2, 128.7, 129.0, 130.2, 137.2, 140.3, 141.6, 142.5, 143.3, 144.1, 154.0, 155.8, 156.3, 161.0, 161.2, 189.3. HRMS-TOF: *m*/*z* $[M+Na]^+$ 562.1585 (Calcd for $C_{30}H_{25}N_3NaO_7$: 562.1585).

4.5.5. (E)-7-((1-(4-(3-(2,3,4-trimethoxyphenyl)acryloyl)phenyl)-1H-1,2,3-triazol-4-yl)methoxy)-2H-chromen-2-one (**13**)

Starting from azidochalcone **7e** and alkyne **8a**. Yellow solid. 50%. mp 221–222 °C. IR (UATR) cm^{-1}: 1737, 1658, 1623, 1605, 1499, 1464. ^{1}H NMR (300 MHz, $CDCl_3$) δ 3.92, 3.94, 3.98 (3s, 9H, 3 × OCH_3), 5.39 (s, 2H, CH_2O), 6.30 (d, *J* = 9.6 Hz, 1H, C3), 6.76 (d, *J* = 8.8 Hz, 1H, C5″-Ar*H*), 6.96–7.02 (m, 2H, C6 and C8), 7.40–7.47 (m, 2H, C5 and C6″-Ar*H*), 7.58 (d, *J* = 15.8 Hz, 1H, CH=C*H*CO), 7.67 (d, *J* = 9.5 Hz, 1H, C4), 7.93 (d, *J* = 8.8 Hz, 2H, C3′-Ar*H* and C5′-Ar*H*), 8.06 (d, *J* = 15.8 Hz, 1H, C*H*=CHCO), 8.20 (d, *J* = 8.8 Hz, 2H, C2′-Ar*H* and C6′-Ar*H*), 8.22 (s, 1H, C*H*N). ^{13}C NMR (75 MHz, $CDCl_3$) δ 56.1, 60.9, 61.4, 62.2, 102.2, 107.7, 112.7, 113.2, 113.7, 120.2, 120.6, 121.0, 121.7, 124.2, 129.0, 130.2, 130.6, 138.8, 139.4, 141.3, 142.5, 143.2, 144.2, 154.0, 155.8, 156.2, 161.0, 161.2, 189.3. HRMS-TOF: *m*/*z* $[M+H]^+$ 540.1767 (Calcd for $C_{30}H_{26}N_3O_7$: 540.1765).

4.5.6. (E)-7-((1-(4-(3-(3,4,5-trimethoxyphenyl)acryloyl)phenyl)-1H-1,2,3-triazol-4-yl)methoxy)-2H-chromen-2-one (**14**)

Starting from azidochalcone **7f** and alkyne **8a**. Yellow solid. 87%. mp 223–224 °C. IR (UATR) cm^{-1}: 1705, 1662, 1606, 1580, 1502. ^{1}H NMR (300 MHz, DMSO-d_6) δ 3.72, 3.87 (2s, 9H, 3 × OCH_3), 5.40 (s, 2H, CH_2O), 6.32 (d, *J* = 9.5 Hz, 1H, C3), 7.07 (d, *J* = 8.6 Hz, 1H, C6), 7.22 (s, 1H, C8), 7.26 (s, 2H, C2″-Ar*H* and C6″-Ar*H*), 7.67 (d, *J* = 8.6 Hz, 1H, C5), 7.75 (d, *J* = 15.5 Hz, 1H, CH=C*H*CO), 7.95 (d, *J* = 15.5 Hz, 1H, C*H*=CHCO), 7.99 (d, *J* = 9.6 Hz, 1H, C4), 8.14 (d, *J* = 8.4 Hz, 2H, C3′-Ar*H* and C5′-Ar*H*), 8.39 (d, *J* = 8.4 Hz, 2H, C2′-Ar*H* and C6′-Ar*H*), 9.16 (s, 1H, C*H*N). ^{13}C NMR (75 MHz, DMSO-d_6) δ 56.7, 60.6, 62.0, 102.1, 107.2, 113.2, 113.3, 113.4, 120.5, 121.5, 123.8, 126.9, 130.1, 130.6, 130.9, 137.9, 139.9, 140.4, 144.0, 144.7, 145.6, 153.6, 155.8, 160.7, 161.5, 188.5. HRMS-TOF: *m*/*z* $[M+Na]^+$ 562.1569 (Calcd for $C_{30}H_{25}N_3NaO_7$: 562.1585).

4.5.7. (E)-4-((1-(3-(3-(3,4-dimethoxyphenyl)acryloyl)phenyl)-1H-1,2,3-triazol-4-yl)methoxy)-2H-chromen-2-one (**15**)

Starting from azidochalcone **7a** and alkyne **8b**. Yellow solid. 62%. mp 201–202 °C. IR (UATR) cm^{-1}: 1713, 1660, 1622, 1609, 1568, 1510, 1454. ^{1}H NMR (300 MHz, $CDCl_3$) δ 3.96, 3.98 (2s, 6H, 2 × OCH_3), 5.47 (s, 2H, CH_2O), 5.94 (s, 1H, C3), 6.93 (d, *J* = 8.3 Hz, 1H, C5″-Ar*H*), 7.20 (s, 1H, C2″-Ar*H*), 7.24–7.37 (m, 3H, C6, C8 and C6″-Ar*H*), 7.44 (d, *J* = 15.6 Hz, 1H, CH=C*H*CO), 7.57 (t, *J* = 8.4 Hz, 1H, C7), 7.73 (t, *J* = 7.9 Hz, 1H, C5′-Ar*H*), 7.87 (d, *J* = 7.9 Hz, 1H, C5), 7.87 (d, *J* = 15.8 Hz, 1H, C*H*=CHCO), 8.03 (d, *J* = 8.0 Hz, 1H, C4′-Ar*H*), 8.13 (d, *J* = 7.7 Hz, 1H, C6′-Ar*H*), 8.33 (s, 1H, C*H*N), 8.39 (s, 1H, C2′-Ar*H*). ^{13}C NMR (75 MHz, $CDCl_3$) δ 56.1, 62.6, 91.3, 110.2, 111.2, 115.4, 116.8, 118.9, 120.1, 121.8, 123.1, 123.7, 124.0, 124.4, 127.4, 128.8, 130.3, 132.6, 137.2, 140.2, 142.6, 146.6, 149.4, 151.9, 153.4, 162.6, 164.9, 188.8. HRMS-TOF: *m*/*z* $[M+Na]^+$ 532.1458 (Calcd for $C_{29}H_{23}N_3NaO_6$: 532.1479).

4.5.8. (E)-4-((1-(3-(3-(2,3-dimethoxyphenyl)acryloyl)phenyl)-1H-1,2,3-triazol-4-yl)methoxy)-2H-chromen-2-one (**16**)

Starting from azidochalcone **7b** and alkyne **8b**. White solid. 88%. mp 137–138 °C. IR (UATR) cm^{-1}: 1713, 1663, 1622, 1608, 1587, 1575, 1478. ^{1}H NMR (300 MHz, $CDCl_3$) δ 3.92 (s, 6H, 2 × OCH_3), 5.47 (s, 2H, CH_2O), 5.94 (s, 1H, C3), 7.02 (dd, *J* = 8.1, 1.2 Hz, 1H, C4″-Ar*H*), 7.14 (t, *J* = 8.0 Hz, 1H, C5″-Ar*H*), 7.25–7.37 (m, 3H, C6, C8 and C6″-Ar*H*), 7.57 (dt, *J* = 7.9, 1.5 Hz, 1H, C7), 7.63 (d, *J* = 15.6 Hz, 1H, CH=C*H*CO), 7.74 (t, *J* = 7.9 Hz, 1H, C5′-Ar*H*), 7.85 (dd, *J* = 7.9, 1.4 Hz, 1H, C5), 8.08–8.17 (m, 2H, C4′-Ar*H* and C6′-Ar*H*), 8.19 (d, *J* = 15.9 Hz, 1H, C*H*=CHCO), 8.32 (t, *J* = 1.7 Hz, 1H, C*H*N), 8.38 (s, 1H, C2′-Ar*H*). ^{13}C NMR (75 MHz, $CDCl_3$) δ 55.9, 61.4, 62.6, 91.3, 114.7, 115.4, 116.8, 119.7, 120.2, 121.7, 122.7, 123.2, 124.0, 124.3, 124.5, 128.7, 128.9, 130.3, 132.6, 137.2, 140.0, 141.2, 149.2, 153.3, 153.4, 162.6, 164.9, 189.3. HRMS-TOF: *m*/*z* $[M+Na]^+$ 532.1476 (Calcd for $C_{29}H_{23}N_3NaO_6$: 532.1479).

4.5.9. (E)-4-((1-(3-(3-(2,3,4-trimethoxyphenyl)acryloyl)phenyl)-1H-1,2,3-triazol-4-yl)methoxy)-2H-chromen-2-one (**17**)

Starting from azidochalcone **7d** and alkyne **8b**. Yellow solid. 79%. mp 198–199 °C. IR (UATR) cm^{-1}: 1713, 1660, 1622, 1609, 1579, 1565, 1494, 1464. ^{1}H NMR (300 MHz, $CDCl_3$) δ 3.93, 3.95, 3.97 (3s, 9H, 3 × OCH_3), 5.47 (s, 2H, CH_2O), 5.94 (s, 1H, C3), 6.76 (d, *J* = 8.8 Hz, 1H, C5″-Ar*H*), 7.28 (dt, *J* = 7.6, 1.0 Hz, 1H, C6), 7.35 (d, *J* = 8.4 Hz, 1H, C8), 7.44 (d, *J* = 8.8 Hz, 1H, C6″-Ar*H*), 7.58 (dt, *J* = 7.8, 1.6 Hz, 1H, C7), 7.59 (d, *J* = 15.8 Hz, 1H, CH=C*H*CO), 7.73 (t, *J* = 7.9 Hz, 1H, C5′-Ar*H*), 7.85 (dd, *J* = 7.9, 1.5 Hz, 1H, C5), 8.09 (d, *J* = 15.8 Hz, 1H, C*H*=CHCO), 8.08–8.16 (m, 2H, C4′-Ar*H* and C6′-Ar*H*), 8.32 (s, 1H, C*H*N), 8.38 (t, *J* = 1.7 Hz, 1H, C2′-Ar*H*). ^{13}C NMR (75 MHz, $CDCl_3$) δ 56.1, 61.0, 61.5, 62.6, 91.3, 107.7, 115.4, 116.8, 120.2, 120.3, 121.6, 121.7, 123.2, 124.0, 124.2, 124.3, 128.9, 130.3, 132.6, 137.1, 140.3, 141.7, 142.5, 153.4, 154.0, 156.3, 162.6, 165.0, 189.3. HRMS-TOF: *m*/*z* $[M+Na]^+$ 562.1591 (Calcd for $C_{30}H_{25}N_3NaO_7$: 562.1585).

4.5.10. (E)-4-((1-(4-(3-(2,3,4-trimethoxyphenyl)acryloyl)phenyl)-1H-1,2,3-triazol-4-yl)methoxy)-2H-chromen-2-one (**18**)

Starting from azidochalcone **7e** and alkyne **8b**. Yellow solid. 70%. mp 151–152 °C. IR (UATR) cm^{-1}: 1717, 1660, 1621, 1606, 1563, 1494, 1464. ^{1}H NMR (300 MHz, $CDCl_3$) δ 3.88, 3.91, 3.95 (3s, 9H, 3 × OCH_3), 5.43 (s, 2H, CH_2O), 5.90 (s, 1H, C3), 6.73 (d, *J* = 8.8 Hz, 1H, C5″-Ar*H*),

7.25 (t, J = 7.2 Hz, 1H, C6), 7.31 (d, J = 8.3 Hz, 2H, C8), 7.40 (d, J = 8.8 Hz, 1H, C6″-Ar*H*), 7.54 (t, J = 7.3 Hz, 1H, C7), 7.55 (d, J = 15.8 Hz, 1H, CH=C*H*CO), 7.80 (d, J = 7.8 Hz, 1H, C5), 7.92 (d, J = 8.6 Hz, 2H, C3′-Ar*H* and C5′-Ar*H*), 8.03 (d, J = 15.8 Hz, 1H, C*H*=CHCO), 8.18 (d, J = 8.6 Hz, 2H, C2′-Ar*H* and C6′-Ar*H*), 8.29 (s, 1H, C*H*N). ^{13}C NMR (75 MHz, $CDCl_3$) δ 56.1, 61.0, 61.5, 62.5, 91.4, 107.7, 115.4, 116.8, 120.3, 120.6, 121.7, 123.1, 124.0, 124.2, 130.3, 132.7, 139.0, 139.3, 141.4, 153.4, 154.0, 156.2, 162.5, 164.9, 189.3. HRMS-TOF: m/z $[M+H]^+$ 540.1776 (Calcd for $C_{30}H_{26}N_3O_7$: 540.1765).

4.5.11. (*E*)-4-((1-(4-(3-(3,4,5-trimethoxyphenyl)acryloyl)phenyl)-1*H*-1,2,3-triazol-4-yl)methoxy)-2*H*-chromen-2-one (**19**)

Starting from azidochalcone **7f** and alkyne **8b**. Yellow solid. 86%. mp 229–230 °C. IR (UATR) cm^{-1}: 1712, 1687, 1659, 1623, 1606, 1583, 1505, 1455. ^{1}H NMR (300 MHz, DMSO-d_6) δ 3.72, 3.88 (2s, 9H, 3 × OC*H*$_3$), 5.56 (s, 2H, C*H*$_2$O), 6.22 (s, 1H, C3), 7.27 (s, 2H, C2″-Ar*H* and C6″-Ar*H*), 7.36 (t, J = 7.7 Hz, 1H, C6), 7.42 (d, J = 8.3 Hz, 1H, C8), 7.67 (dt, J = 8.3, 1.4 Hz, 1H, C7), 7.76 (d, J = 15.5 Hz, 1H, CH=C*H*CO), 7.85 (dd, J = 7.8, 1.2 Hz, 1H, C5), 7.96 (d, J = 15.6 Hz, 1H, C*H*=CHCO), 8.18 (d, J = 8.6 Hz, 2H, C3′-Ar*H* and C5′-Ar*H*), 8.40 (d, J = 8.7 Hz, 2H, C2′-Ar*H* and C6′-Ar*H*), 9.25 (s, 1H, C*H*N). ^{13}C NMR (75 MHz, DMSO-d_6) δ 56.7, 60.6, 63.2, 92.0, 107.2, 115.5, 116.9, 120.6, 121.5, 123.5, 124.1, 124.7, 130.6, 130.9, 133.4, 138.0, 139.9, 143.1, 145.6, 153.3, 153.6, 162.0, 164.8, 188.5. HRMS-TOF: m/z $[M+Na]^+$ 562.1581 (Calcd for $C_{30}H_{25}N_3NaO_7$: 562.1585).

4.6. Cytotoxic assay: cancer cell lines

The cells suspended in the corresponding culture medium were inoculated in 96-well microtiter plates (Corning Inc., NY, USA) at a density of 10,000–20,000 cells per well, and incubated for 24 h at 37 °C in a humidified atmosphere with 95% air and 5% CO_2. An equal volume of additional medium containing either the serial dilutions of the test compounds, positive control (etoposide and/or doxorubicin), or negative control (DMSO) was added to the desired final concentrations, and the microtiter plates were further incubated for an additional 48 h. The number of surviving cells in each well was determined using MTT assay [47,48] (for adherent cells: HuCCA-1, HepG2, and A549 cells) and XTT assay [49] (for suspended cells: MOLT-3 cells). The IC_{50} value is defined as the drug (or compound) concentration that inhibits cell growth by 50% (relative to negative control).

4.7. Antimalarial assay: radioisotope techniques

P. falciparum (K1, multidrug resistant strain) was cultivated *in vitro* conditions, according to Trager & Jensen (1976) [50], in RPMI 1640 medium containing 20 mM HEPES (*N*-2-hydroxyethylpiperazine-*N*′-2-ethanesulfonic acid), 32 mM $NaHCO_3$ and 10% heat activated human serum with 3% erythrocytes, in humidified 37 °C incubator with 3% CO_2. The culture was passaged with fresh mixture of erythrocytes and medium for every day to maintain cell growth. Quantitative assessment of antimalarial activity *in vitro* was determined by microculture radioisotope techniques based upon the methods described by Desjardins et al. (1979) [51]. Briefly, a mixture of 200 μL of 1.5% erythrocytes with 1% parasitemia at the early ring stage was pre-exposed to 25 μL of the medium containing a test sample dissolved in 1% DMSO (0.1% final concentration) for 24 h. Subsequently, 25 μL of [3H] hypoxanthine (Amersham, USA) in culture medium (0.5 μCi) was added to each well and the plates were incubated for an additional 24 h. Levels of incorporated radioactive labeled hypoxanthine, indicating parasite growth, were determined using the Top Count microplate scintillation counter (Packard, USA). The percentage of parasite growth was calculated using the signal count per minute of treated (CPMT) and untreated conditions (CPMU) as shown by the following equation;

$$\%\ \text{parasite growth} = \text{CPMT}/\text{CPMU} \times 100$$

4.8. Cytotoxicity assay: primate cell line (Vero)

The cytotoxicity assay was performed using the Green Fluorescent Protein (GFP) detection method [52]. The GFP-expressing Vero cell line was generated in-house by stably transfecting the African green monkey kidney cell line (Vero, ATCC CCL-81), with pEGFP-N1 plasmid (Clontech). The cell line was maintained in a minimal essential medium supplemented with 10% heat-inactivated fetal bovine serum, 2 mM L-glutamine, 1 mM sodium pyruvate, 1.5 g/L sodium bicarbonate and 0.8 mg/mL geneticin, at 37 °C in a humidified incubator with 5% CO_2. The assay was carried out by adding 45 μL of cell suspension at 3.3×10^4 cells/mL to each well of 384-well plates containing 5 μL of test compounds previously diluted in 0.5% DMSO, and then incubating for 4 days at 37 °C incubator with 5% CO_2. Fluorescence signals were measured by using SpectraMax M5 microplate reader (Molecular Devices, USA) in the bottom reading mode with excitation and emission wavelengths of 485 and 535 nm, respectively. Fluorescence signal at day 4 was subtracted with background fluorescence at day 0. IC_{50} values were derived from dose–response curves, using 6 concentrations of 3-fold serially diluted samples, by the SOFTMax Pro software (Molecular device). Ellipticine and 0.5% DMSO were used as a positive and a negative control, respectively.

4.9. Molecular docking

Molecular docking was performed to investigate the binding modalities of ligands toward possible targets comprising of falcipain-2 (PDB id 3BPF), a cysteine protease from *P. falciparum*, as well as α- and β-tubulin complexes (PDB id 1SA0) from Bos taurus. Protein structures were prepared for docking by adding essential hydrogen atoms and modeling missing side chains using the WHAT IF web server version 10.1a [53]. Furthermore, non-polar hydrogen atoms were merged, Gasteiger atomic charges were assigned, and atom type of receptors were specified using AutoDock Tools version 1.5.6. [54,55]. Chalcone–triazole–coumarin ligands were constructed using Marvin Sketch version 6.1.4 [56] and geometrically optimized with Gaussian 09 [57] at the B3LYP/6-31G(d) level of theory. Ligand structures were prepared for docking by merging non-polar hydrogen atoms and defining rotatable bonds using AutoDock Tools version 1.5.6. Partial atomic charges calculated by Gaussian 09 were assigned to ligands for further use in the docking process. A grid box size of 25.0, 25.0, 25.0 Å was generated and allocated at the center of the receptor binding site using x, y and z coordinates of −91.5906, 5.0925 and −21.4080 for falcipain-2 and 118.4155, 89.6890 and 6.2141 for α- and β-tubulin complexes. Molecular docking simulations were performed using AutoDock Vina as part of the PyRx 0.8 software [58]. Co-crystallized ligands were re-docked as validation of the docking protocol. Docked structures were visualized using PyMOL [59]. Two-dimensional schematic representation of protein-ligand interaction was generated using PoseViewWeb version 1.97.0 [60].

Acknowledgments

This project is supported by the research grants from Srinakharinwirot University under the Government Budget (B.E. 2559). We would like to thank the Thailand Research Fund, the office of the Higher Education Commission, and Srinakharinwirot University

(Grant No. MRG5680001) for financial support. Great supports from the office of the Higher Education Commission and Mahidol University under the National Research Universities Initiative are appreciated. We are also indebted to Chulabhorn Research Institute for recording mass spectra and bioactivity testing.

Appendix A. Supplementary data

Supplementary data related to this article can be found at http://dx.doi.org/10.1016/j.ejmech.2014.07.087.

References

[1] N.K. Sahu, S.S. Balbhadra, J. Choudhary, D.V. Kohli, Exploring pharmacological significance of chalcone scaffold: a review, Curr. Med. Chem. 19 (2012) 209–225.
[2] L. Ni, C.Q. Meng, J.A. Sikorski, Recent advances in therapeutic chalcones, Expert Opin. Ther. Pat. 14 (2004) 1669–1691.
[3] D.I. Batovska, I.T. Todorova, Trends in utilization of the pharmacological potential of chalcones, Curr. Clin. Pharmacol. 5 (2010) 1–29.
[4] J.R. Dimmock, D.W. Elias, M.A. Beazely, N.M. Kandepu, Bioactivities of chalcones, Curr. Med. Chem. 6 (1999) 1125–1149.
[5] M.L. Go, X. Wu, X.L. Liu, Chalcones: an update on cytotoxic and chemoprotective properties, Curr. Med. Chem. 12 (2005) 483–499.
[6] S. Ducki, Antimitotic chalcones and related compounds as inhibitors of tubulin assembly, Anticancer Agents Med. Chem. 9 (2009) 336–347.
[7] C. Dyrager, M. Wickström, M. Fridén-Saxin, A. Friberg, K. Dahlén, E.A.A. Wallén, J. Gullbo, M. Grøtli, K. Luthman, Inhibitors and promoters of tubulin polymerization: synthesis and biological evaluation of chalcones and related dienones as potential anticancer agents, Bioorg. Med. Chem. 19 (2011) 2659–2665.
[8] M. Chen, T.G. Theander, S.B. Christensen, L. Hviid, L. Zhai, A. Kharazmi, Licochalcone A, a new antimalarial agent, inhibits *in vitro* growth of the human malaria parasite *Plasmodium falciparum* and protects mice from *P. yoelii* infection, Antimicrob. Agents Chemother. 38 (1994) 1470–1475.
[9] N. Sriwilaijaroen, M. Liu, M.-L. Go, P. Wilairat, Plasmepsin II inhibitory activity of alkoxylated and hydroxylated chalcones, Southeast Asian J. Trop. Med. Public Health 37 (2006) 607–612.
[10] G. Wanare, R. Aher, N. Kawathekar, R. Ranjan, N.K. Kaushik, D. Sahal, Synthesis of novel alpha-pyranochalcones and pyrazoline derivatives as *Plasmodium falciparum* growth inhibitors, Bioorg. Med. Chem. Lett. 420 (2010) 4675–4678.
[11] R. Li, G.L. Kenyon, F.E. Cohen, X. Chen, B. Gong, J.N. Dominguez, E. Davidson, G. Kurzban, R.E. Miller, E.O. Nuzum, P.J. Rosenthal, J.H. McKerrow, *In vitro* antimalarial activity of chalcones and their derivatives, J. Med. Chem. 38 (1995) 5031–5037.
[12] R.H. Hans, J. Gut, P.J. Rosenthal, K. Chibale, Comparison of the antiplasmodial and falcipain-2 inhibitory activity of β-amino alcohol thiolactone-chalcone and isatin-chalcone hybrids, Bioorg. Med. Chem. Lett. 20 (2010) 2234–2237.
[13] J.A. Geyer, S.M. Keenan, C.L. Woodard, P.A. Thompson, L. Gerena, D.A. Nichols, C.E. Gutteridge, N.C. Waters, Selective inhibition of Pfmrk, a *Plasmodium falciparum* CDK, by antimalarial 1,3-diaryl-2-propenones, Bioorg. Med. Chem. Lett. 19 (2009) 1982–1985.
[14] M.-L. Go, M. Liu, P. Wilairat, P.J. Rosenthal, K.J. Saliba, K. Kirk, Antiplasmodial chalcones inhibit sorbitol-induced hemolysis of *Plasmodium falciparum*-infected erythrocytes, Antimicrob. Agents Chemother. 48 (2004) 3241–3245.
[15] M. Larsen, H. Kromann, A. Kharazmi, S.F. Nielsen, Conformationally restricted anti-plasmodial chalcones, Bioorg. Med. Chem. Lett. 15 (2005) 4858–4861.
[16] M. Liu, P. Wilairat, M.-L. Go, Antimalarial alkoxylated and hydroxylated chalcones: structure-activity relationship analysis, J. Med. Chem. 44 (2001) 4443–4452.
[17] F. Borges, F. Roleira, N. Milhazes, L. Santana, E. Uriarte, Simple coumarins and analogues in medicinal chemistry: occurrence, synthesis and biological activity, Curr. Med. Chem. 12 (2005) 887–916.
[18] I. Kostova, Synthetic and natural coumarins as cytotoxic agents, Curr. Med. Chem. Anticancer Agents 5 (2005) 29–46.
[19] A. Lacy, R. O'Kennedy, Studies on coumarins and coumarin-related compounds to determine their therapeutic role in the treatment of cancer, Curr. Pharm. Des. 10 (2004) 3797–3811.
[20] Coumarins. Biology, Applications and Mode of Action, Wiley, New York, 1997.
[21] Y.-Z. Yang, A. Ranz, H.-Z. Pan, Z.-N. Zhang, X.-B. Lin, S.R. Meshnick, Daphnetin: a novel antimalarial agent with *in vitro* and *in vivo* activity, Am. J. Trop. Med. Hyg. 46 (1992) 15–20.
[22] K. Nepali, S. Sharma, M. Sharma, P.M.S. Bedi, K.L. Dhar, Rational approaches, design strategies, structure activity relationship and mechanistic insights for anticancer hybrids, Eur. J. Med. Chem. 77 (2014) 422–487.
[23] F.W. Muregi, A. Ishih, Next-generation antimalarial drugs: hybrid molecules as a new strategy in drug design, Drug Dev. Res. 71 (2010) 20–32.
[24] C. Hubschwerlen, J.L. Specklin, C. Sigwalt, S. Schroeder, H.H. Locher, Design, synthesis and biological evaluation of oxazolidinone-quinolone hybrids, Bioorg. Med. Chem. 11 (2003) 2313–2319.
[25] R. Pingaew, S. Prachayasittikul, S. Ruchirawat, V. Prachayasittikul, Synthesis and cytotoxicity of novel 4-(4-(substituted)-1*H*-1,2,3-triazol-1-yl)-*N*-phenethylbenzenesulfonamides, Med. Chem. Res. 23 (2014) 1768–1780.
[26] E.M. Guantai, K. Ncokazi, T.J. Egan, J. Gut, P.J. Rosenthal, P.J. Smith, K. Chibale, Design, synthesis and *in vitro* antimalarial evaluation of triazole-linked chalcone and dienone hybrid compounds, Bioorg. Med. Chem. 18 (2010) 8243–8256.
[27] K.V. Sashidhara, S.R. Avula, G.R. Palnati, S.V. Singh, K. Srivastava, S.K. Puri, J.K. Saxena, Synthesis and *in vitro* evaluation of new chloroquine-chalcone hybrids against chloroquine-resistant strain of *Plasmodium falciparum*, Bioorg. Med. Chem. Lett. 22 (2012) 5455–5459.
[28] K.V. Sashidhara, M. Kumar, R.K. Modukuri, R.K. Srivastava, A. Soni, K. Srivastava, S.V. Singh, J.K. Saxena, H.M. Gauniyal, S.K. Puri, Antiplasmodial activity of novel keto-enamine chalcone-chloroquine based hybrid pharmacophores, Bioorg. Med. Chem. 20 (2012) 2971–2981.
[29] A. Kamal, S. Prabhakar, M.J. Ramaiah, P.V. Reddy, Ch.R. Reddy, A. Mallareddy, N. Shankaraiah, T.L.N. Reddy, S.N.C.V.L. Pushpavalli, M. Pal-Bhadra, Synthesis and anticancer activity of chalcone-pyrrolobenzodiazepine conjugates linked *via* 1,2,3-triazole ring side-armed with alkane spacers, Eur. J. Med. Chem. 46 (2011) 3820–3831.
[30] M. Abdel-Aziz, S.-E. Park, G.E.-D.A.A. Abuo-Rahma, M.A. Sayed, Y. Kwon, Novel *N*-4-piperazinyl-ciprofloxacin-chalcone hybrids: synthesis, physicochemical properties, anticancer and topoisomerase I and II inhibitory activity, Eur. J. Med. Chem. 69 (2013) 427–438.
[31] P. Singh, R. Raj, V. Kumar, M.P. Mahajan, P.M.S. Bedi, T. Kaur, A.K. Saxena, 1,2,3-Triazole tethered β-lactam-chalcone bifunctional hybrids: synthesis and anticancer evaluation, Eur. J. Med. Chem. 47 (2012) 594–600.
[32] M.A.E. Mourad, M. Abdel-Aziz, G.E.-D.A.A. Abuo-Rahma, H.H. Farag, Design, synthesis and anticancer activity of nitric oxide donating/chalcone hybrids, Eur. J. Med. Chem. 54 (2012) 907–913.
[33] X. Dong, L. Du, Z. Pan, T. Liu, B. Yang, Y. Hu, Synthesis and biological evaluation of novel hybrid chalcone derivatives as vasorelaxant agents, Eur. J. Med. Chem. 45 (2010) 3986–3992.
[34] F. Pérez-Cruz, S. Vazquez-Rodriguez, M.J. Matos, A. Herrera-Morales, F.A. Villamena, A. Das, B. Gopalakrishnan, C. Olea-Azar, L. Santana, E. Uriarte, Synthesis and electrochemical and biological studies of novel coumarin-chalcone hybrid compounds, J. Med. Chem. 56 (2013) 6136–6145.
[35] S. Vazquez-Rodriguez, R. Figueroa-Guíñez, M.J. Matos, L. Santana, E. Uriarte, M. Lapier, J.D. Maya, C. Olea-Azar, Synthesis of coumarin-chalcone hybrids and evaluation of their antioxidant and trypanocidal properties, MedChemComm 4 (2013) 993–1000.
[36] K.V. Sashidhara, M. Kumar, R.K. Modukuri, R. Sonkar, G. Bhatia, A.K. Khanna, S. Rai, R. Shukla, Synthesis and anti-inflammatory activity of novel biscoumarin–chalcone hybrids, Bioorg. Med. Chem. Lett. 21 (2011) 4480–4484.
[37] E. Bombardelli, P. Valenti, Preparation of 8-(Arylpropenoyl)coumarins as Antiproliferative Agents. PCT Int. Pub. No. WO 01/17984 A1, 2001.
[38] K.V. Sashidhara, A. Kumar, M. Kumar, J. Sarkar, S. Sinha, Synthesis and *in vitro* evaluation of novel coumarin-chalcone hybrids as potential anticancer agents, Bioorg. Med. Chem. Lett. 20 (2010) 7205–7211.
[39] K. Patel, C. Karthikeyan, N.S. Hari Narayana Moorthy, G.S. Deora, V.R. Solomon, H. Lee, P. Trivedi, Design, synthesis and biological evaluation of some novel 3-cinnamoyl-4-hydroxy-2*H*-chromen-2-ones as antimalarial agents, Med. Chem. Res. 21 (2012) 1780–1784.
[40] S.G. Agalave, S.R. Maujan, V.S. Pore, Click chemistry: 1,2,3-triazoles as pharmacophores, Chem. Asian J. 6 (2011) 2696–2718.
[41] I.D. Kerr, J.H. Lee, K.C. Pandey, A. Harrison, M. Sajid, P.J. Rosenthal, L.S. Brinen, Structures of falcipain-2 and falcipain-3 bound to small molecule inhibitors: implications for substrate specificity, J. Med. Chem. 52 (2009) 852–857.
[42] V. Prachayasittikul, S. Prachayasittikul, S. Ruchirawat, V. Prachayasittikul, 8-Hydroxyquinolines: a review of their metal chelating properties and medicinal applications, Drug Des. Dev. Ther. 7 (2013) 1157–1178.
[43] J. Wu, J. Li, Y. Cai, Y. Pan, F. Ye, Y. Zhang, Y. Zhao, S. Yang, X. Li, G. Liang, Evaluation and discovery of novel synthetic chalcone derivatives as anti-inflammatory agents, J. Med. Chem. 54 (2011) 8110–8123.
[44] Y.R. Prasad, A.S. Rao, R. Rambabu, Synthesis of some 4′-amino chalcones and their antiinflammatory and antimicrobial activity, Asian J. Chem. 21 (2009) 907–914.
[45] I. Kosiova, S. Kovackova, P. Kois, Synthesis of coumarin–nucleoside conjugates *via* Huisgen 1,3-dipolar cycloaddition, Tetrahedron 63 (2007) 312–320.
[46] C.P. Rao, G. Srimannarayana, Claisen rearrangement of 4-propargloxycoumarins: formation of 2*H*,5*H*-Pyrano[3,2-*c*][1]benzopyran-5-ones, Syn. Comm. 20 (1990) 535–540.
[47] J. Carmichael, W.G. DeGraff, A.F. Gazdar, J.D. Minna, J.B. Mitchell, Evaluation of a tetrazolium-based semiautomated colorimetric assay: assessment of radiosensitivity, Cancer Res. 47 (1987) 943–946.
[48] T. Mosmann, Rapid colorimetric assay for cellular growth and survival: application to proliferation and cytotoxicity assays, J. Immunol. Methods 65 (1983) 55–63.
[49] A. Doyle, J.B. Griffiths, Mammalian Cell Culture: Essential Techniques, John Wiley & Sons, Chichester, UK, 1997.
[50] W. Trager, J.B. Jensen, Human malaria parasites in continuous culture, Science 193 (1976) 673–675.
[51] R.E. Desjardins, C.J. Canfield, J.D. Haynes, J.D. Chulay, Quantitative assessment of antimalarial activity *in vitro* by a semiautomated microdilution technique, Antimicrob. Agents Chemother. 16 (1979) 710–718.

[52] L. Hunt, M. Jordan, M. De Jesus, F.M. Wurm, GFP-expressing mammalian cells for fast, sensitive, noninvasive cell growth assessment in a kinetic mode, Biotechnol. Bioeng. 65 (1999) 201–205.
[53] R. Rodriguez, G. Chinea, N. Lopez, T. Pons, G. Vriend, Homology modeling, model and software evaluation: three related resources, Bioinformatics 14 (1998) 523–528.
[54] M.F. Sanner, Python: a programming language for software integration and development, J. Mol. Graph. Mod. 17 (1999) 57–61.
[55] G.M. Morris, R. Huey, W. Lindstrom, M.F. Sanner, R.K. Belew, D.S. Goodsell, A.J. Olson, Autodock4 and AutoDockTools4: automated docking with selective receptor flexibility, J. Comput. Chem. 16 (2009) 2785–2791.
[56] ChemAxon Marvin Sketch Version 6.0, 2013 (Budapest, Hungary).
[57] M.J. Frisch, G.W. Trucks, H.B. Schlegel, G.E. Scuseria, M.A. Robb, J.R. Cheeseman, G. Scalmani, V. Barone, B. Mennucci, G.A. Petersson, H. Nakatsuji, M. Caricato, X. Li, H.P. Hratchian, A.F. Izmaylov, J. Bloino, G. Zheng, J.L. Sonnenberg, M. Hada, M. Ehara, K. Toyota, R. Fukuda, J. Hasegawa, M. Ishida, T. Nakajima, Y. Honda, O. Kitao, H. Nakai, T. Vreven, J.A. Montgomery, J.E. Peralta, F. Ogliaro, M. Bearpark, J.J. Heyd, E. Brothers, K.N. Kudin, V.N. Staroverov, R. Kobayashi, J. Normand, K. Raghavachari, A. Rendell, J.C. Burant, S.S. Iyengar, J. Tomasi, M. Cossi, N. Rega, J.M. Millam, M. Klene, J.E. Knox, J.B. Cross, V. Bakken, C. Adamo, J. Jaramillo, R. Gomperts, R.E. Stratmann, O. Yazyev, A.J. Austin, R. Cammi, C. Pomelli, J.W. Ochterski, R.L. Martin, K. Morokuma, V.G. Zakrzewski, G.A. Voth, P. Salvador, J.J. Dannenberg, S. Dapprich, A.D. Daniels, Farkas, J.B. Foresman, J.V. Ortiz, J. Cioslowski, D.J. Fox, Gaussian 09, 2009 (Wallingford, Connecticut).
[58] S. Dallakyan, PyRx Version 0.8, 2013. http://pyrx.scripps.edu.
[59] W. Delano, PyMOL Release 0.99, DeLano Scientific LLC, Palo Alto, CA, 2002.
[60] K. Stierand, M. Rarey, Drawing the PDB: protein-ligand complexes in two dimensions, ACS Med. Chem. Lett. 1 (2010) 540–545.